

LARGE-SCALE GRAPHENE TRANSFER IN ULTRA-HIGH VACUUM
AND
DESIGN OF A LOW TEMPERATURE ULTRA-HIGH VACUUM
SCANNING TUNNELING MICROSCOPE

BY

XIMENG LIU

THESIS

Submitted in partial fulfillment of the requirements
for the degree of Master of Science in Electrical and Computer Engineering
in the Graduate College of the
University of Illinois at Urbana-Champaign, 2014

Urbana, Illinois

Adviser:

Professor Joseph W. Lyding

ABSTRACT

This thesis documents a way of transferring large-scale graphene onto clean surfaces in an ultra-high vacuum scanning tunneling microscope chamber via a modified direct contact transfer method. A polyethylene terephthalate (PET) film was chosen as the material for supporting graphene during the in-situ transfer. Both a scanning electron microscope and an atomic force microscope were used to characterize the transferred graphene quality. This is the first demonstration of successfully transferring large-scale graphene in the ultra-high vacuum environment, which opens a lot of opportunities for studying the properties of pristine graphene and graphene-substrate interactions.

Secondly, this thesis also documents an ongoing design and construction of a low temperature, ultra-high vacuum scanning tunneling microscope. A novel cooling mechanism was implemented in our design which includes a closed-cycle refrigerator in order to enable longer experiment durations and reduced costs of operation. So far we are able to reach a temperature of ~30 K with the STM scanner, vibration isolation and all electronic connections installed. We believe that this can be further improved by making some minor modifications to our design as our future work in order to reach our goal of operating at a temperature of <10 K.

ACKNOWLEDGMENTS

I would like to convey my deepest gratitude to Professor Joseph W. Lyding, who took me under his wing while I was still an undergraduate with no idea where I wanted to go with a degree in ECE. He opened the doors to this overwhelming world of nanotechnology and scanning tunneling microscopy and showed me what it took to observe the smallest things in this world. Professor Lyding was always patient, thorough and persistent. He taught me to think outside the box and trust my instincts. He has truly played an indispensable part in my master's studies and I am very happy that I can continue working with him for pursuing my Ph.D. degree.

I am grateful to Dr. Kevin He for his guidance in designing the low temperature STM and training on running experiments on STM. He was calm, knowledgeable and always eager to help. He always made it a priority for me to understand what we were doing before we started. I couldn't have asked for a better mentor and labmate.

I would also like to thank all the members in Lyding's group for their help in conducting experiments and sharing their knowledge: Dr. Scott Schnucker, Dr. Josh Wood, Justin Koepke, Jae Won Do, Adrian Radocea, Yaofeng Chen, Sundaravadivel Rajarajan, Aniruddh Rangarajan, Torin Kilpatrick, and Pam Martin. Being friends with them made my life more enjoyable.

Finally, I would like to thank my family, my fiancé and friends for supporting me all these years. Even when other girls my age were getting jobs, married or even children, they always stood beside me and let me know that I made the right choice.

CONTENTS

CHAPTER 1. INTRODUCTION	1
CHAPTER 2. LARGE-SCALE TRANSFER OF GRAPHENE ONTO CLEAN SURFACES IN ULTRA-HIGH VACUUM	12
CHAPTER 3. DESIGN OF A LOW TEMPERATURE ULTRA-HIGH VACUUM SCANNING TUNNELING MICROSCOPE.....	30
CHAPTER 4. SUMMARY AND OUTLOOK.....	40
REFERENCES	41

CHAPTER 1

INTRODUCTION

1.1 Moore's Law and Nanomaterials

The development of the semiconductor industry has been guided by a famous law predicted by Gordon E. Moore since the late 20th century: the number of transistors in a dense integrated circuit doubles approximately every two years [1]. Starting with the success of growing single crystal silicon [2] and the invention of transistors [3], researchers and companies have tried hard to sustain Moore's law and push the technology forward. However, with the demand of more and more transistors integrated together, the size of each transistor needs to keep shrinking and problems start to appear when transistor size reaches as low as the nanometer scale; one example is Si-MOSFETs, which suffer from current leakage [4] and short channel effect [5], and another is UV-lithography reaching the limit [6].

With the discovery of fullerenes [7] and the invention of instruments that are capable of characterizing materials at nanoscale such as scanning tunneling microscope [8], it is believed that nanomaterials such as graphene [9], carbon nanotube [10] and boron nitride [11], with their outstanding properties, have great potential to ultimately replace Si in the semiconductor industry.

1.2 Graphene

1.2.1 Graphene Structure and Properties

Graphene is a single layer of graphite, made of one sheet of sp^2 bonded carbon atoms in a honeycomb lattice as shown in Figure 1.1 [12]. Graphite is a common material and can be seen

daily in many products such as pencils. However, due to the difficulty of isolating a single layered graphene from the graphite, the study of graphene was only theoretical before the 21st century, and it had even been predicted that no such 2D material would stably exist under room temperature [13]. In October of 2004, one paper [14] about graphene isolation published by Andre Geim and Kostantin Novoselov disproved the prediction and triggered the study of graphene science. They exfoliated a graphite sample multiple times onto a SiO₂ substrate using Scotch tape until small graphene flakes were obtained and modulated the graphene's Fermi level [15]. The success of isolating graphene won them the Nobel Prize and also enabled the discoveries of many exceptional properties of graphene later on, including high electron mobility (200,000cm²V⁻¹s⁻¹ for suspended graphene [16]), high thermal conductivity (twice as much as diamond [17]), high optical transparency (absorbing only ~2% of white light[18]) and high Young's modulus [19]. These properties arise from strong covalent bonds between carbon atoms, σ bonds formed by in-plane hybridized sp² orbitals and π bonds formed by out-of-plane unhybridized p orbital [20], which generates a unique band structure with zero bandgap at the Dirac point and a linear dispersion relation [15] around the Fermi level as shown in Figure 1.2 [21]. All of these characteristics make graphene a great candidate for making electronic devices and even to replace Si as the future wonder material in the semiconductor industry since graphene nanoribbons can have a bandgap [22].

1.2.2 Graphene Transfer Methods

Since graphene is a 2D material, it is mostly served as a thin film deposited onto different substrates such as Si [23] and GaAs [24]. Thus a method of removing it from its original growth substrate and placing it onto the desired substrate with the least damage and contamination is desired. Graphene grown on metals via chemical vapor deposition (CVD) is so far the most

promising method of getting large-scale graphene [23]. The most conventional method of transferring CVD grown graphene for research studies is the wet transfer method [25] (process shown in Figure 1.3 [26]), which involves a wet chemical etching of the metals on which graphene grows with a layer of polymer such as poly (methyl methacrylate) (PMMA) coated on top of graphene. With the protection of such a polymer layer, wafer-scale graphene has been transferred successfully. However, contaminants induced during this process cannot be avoided. Firstly, Cu and Fe ions in the etching solution can adsorb on graphene and change its Fermi level [27]. Secondly, even after dissolving in the acetone solvent and the high temperature Ar/H₂ annealing, PMMA residues still cannot be removed completely [28]. Last but not the least, water can be trapped between the graphene and the substrate during the wet transfer process [29], affecting the interactions between the graphene and the substrate.

One method of transferring graphene without PMMA is to use a thermal release tape (TRT). Samsung has developed a roll-to-roll technique which uses TRT (instead of PMMA) as the support during etching and releases graphene from it by heating above the release temperature [30]. The advantages of this method are low cost, high throughput and no PMMA residue induced. However, this process induces adhesive residues which are also hard to remove and the continuity of graphene after transferring is poor - holes and cracks are introduced [31].

Other than TRT, researchers have also demonstrated graphene transfer using polydimethylsiloxane (PDMS) [32]. PDMS is used for conformal contact with graphene by either pouring liquid PDMS on graphene and curing it or pressing solid PDMS against graphene with enough force. After etching off the metal, the graphene/PDMS can stamp on any arbitrary substrate and then graphene can be detached from the PDMS by mechanically peeling off the PDMS. The adhesion strength between graphene and the PDMS can be controlled by the mixing

ratio of the curing agent [33]. Compared to PMMA and TRT, PDMS leaves little contamination and it can even be utilized with soft substrates [34]. However, due to the strong adhesion force between graphene and the PDMS, it may only work for multilayer and small area graphene transfer and the degree of the continuity of the transferred graphene varies greatly for different substrates [35].

Recently, PDMS has been replaced by a two-layer structure consisting of polyethylene terephthalate (PET) and silicone to transfer graphene [36]. This material is widely used in screen protecting films for smart phones and tablets so it is easy to get. Due to the low surface tension of the silicone, graphene will be released easily and stay clean [36]. And the dispersive adhesion between graphene and silicone enables the recyclable use of PET film. Compared to PDMS, the release time for PET is much shorter and does not require great force.

1.3 Scanning Tunneling Microscope

A scanning tunneling microscope is an instrument for imaging conducting surfaces with atomic resolution in an ultra high vacuum (UHV) environment and is based on the concept of quantum tunneling. As a sharp conducting tip (with radius curvature of sub-nanometer) is brought very close to a conducting surface with a bias applied between the two, electrons can tunnel through the thin vacuum barrier (as shown in Figure 1.4 [37]). The resulting tunneling current is a function of the applied bias, the distance between tip and sample and the local density of states of the sample [8]. Topography of the surface can be obtained by monitoring the change of the tip's position as it scans across the surface with a constant voltage bias and tunneling current. In addition to STM topographic images, scanning tunneling spectroscopy

(STS) can be used to probe the local density of states of the sample. By momentarily disabling the feedback and sweeping the voltage over a specified range while recording the current, a current-voltage spectrum can be obtained which gives the information about the local density of states. Ever since the first STM was invented in 1981 by Gerd Binnig and Heinrich Rohrer [8] and the first image of the Si (111) surface's reconstruction was provided [38], it has served as a powerful tool in the field of surface science.

The STM system used in this work is a homebuilt UHV-STM designed by Professor Joseph Lyding (known as Chamber D). An actual photo of Chamber D is shown in Figure 1.5. This system has three chambers which are isolated by two gate valves: the loadlock, the preparation chamber and the main STM chamber. The loadlock is where we load/unload the samples and it is mainly pumped by a turbo pump to a pressure of $\sim 10^{-8}$ Torr. After the sample is loaded into the loadlock and the turbo vacuum is reached, we open the gate valve between the loadlock and the preparation chamber and use a linear translation manipulator (LTM) to transfer the sample to the preparation chamber. The preparation chamber is pumped by an ion pump to UHV pressure of 10^{-10} - 10^{-11} Torr and it contains a dipstick where the sample degas takes place. Sample degas is an essential sample preparation step for an STM experiment and is realized by running a current across the two leads of the dipstick which are in contact with the sample at the ends. Depending on different types of samples, the degas temperature goes from room temperature to 600 °C. During this heating process, any physisorbed contaminants can be removed from the sample's surface resulting in an ultra-clean surface. Other than sample degas, many other sample preparation processes can also be done in the preparation chamber. For example, we can get a clean Si sample by flashing it at 1250 °C [39] or a hydrogen-passivated (H-passivated) Si surface by leaking H₂ gas into the chamber and cracking it on a hot tungsten

(W) filament [40]. Once the sample is clean and well prepared, it is finally transferred to the STM main chamber via LTM. A STM scanner and a tip/sample garage are sitting on the stage in the STM chamber which is hung by springs to mechanically isolate the vibrations during scan.

1.4 Dry Contact Transfer (DCT) and STM Studies of DCT Graphene on Different Substrates

Developed by Albrecht, a former Ph.D. student from my group, and Professor Lyding, the dry contact transfer (DCT) method for depositing carbon nanotubes on surfaces in UHV [41] was later extended to deposition of exfoliated graphene by Ritter [39]. By firstly exfoliating graphite onto a fiberglass sheath and mounting it to a STM sample holder, nanometer sized graphene was transferred onto a sample surface in an UHV-STM chamber by bringing the fiberglass sheath in contact with the sample surface using the LTM. Dr. Ritter has revealed the relationship between the size of a graphene flake and its electronic band structure by scanning graphene transferred by the DCT method onto an H-passivated Si surface via STM and also showed that this method provides much cleaner graphene edges than transfer in ambient conditions [39].

Later, Dr. He who is also a Lyding group alumnus, conducted a series of STM experiments on graphene transparency for different substrates. By depositing graphene flakes onto an H-passivated Si surface via DCT method, he was able to desorb hydrogen atoms from the silicon surface under the graphene using electrons emitted from the STM tip, resulting in dangling bonds left on the Si surface without damaging the graphene sheet [42]. He hypothesized about the mechanisms by which the electrons could tunnel through the graphene, break the bond

between Si and H atoms and let the H atoms escape from the graphene edges. However, whether electrons can tunnel through the graphene directly from where the beam is emitted or would instead scatter in graphene for a distance and then tunnel through remains as an open question. Different from graphene on Si, he also found a phenomenon where graphene becomes semi-transparent to the STM on GaAs and InAs surfaces [43]. With variable scanning biases, changes in topographic images were observed: at -2 V the GaAs lattice is clearly seen through graphene whereas at -0.6 V only the graphene honeycomb lattice is visible. This phenomenon was explained by a decrease in the tip-sample spacing causing by a large tunneling current that made the tip push the graphene towards the substrate and thus the graphene becomes transparent.

1.5 Thesis Structure

Two ongoing projects constitute this thesis. As an extension of Dr. Ritter and Dr. He's work, Chapter 2 will detail a modified DCT method of transferring large-scale graphene grown on copper onto clean surfaces in a UHV-STM chamber. Different materials that served as the support for graphene will be evaluated. Optical microscope, scanning electron microscope and atomic force microscope images will be presented to characterize the resulting transferred graphene.

Chapter 3 will present an ongoing design and construction of a low temperature, ultra-high vacuum scanning tunneling microscope that is capable of scanning at below 10 K. This was collaboration with Dr. He. Details about the designing of the cooling mechanism which include two boxes and add-ons for the fridge expander for keeping the STM cold have been recorded by Liu in her undergraduate thesis [44]. The assembly procedures of the system including

installation of the vibration isolation, the scanner and the maintenance of the system have been elaborately described by Dr. He in his Ph.D. dissertation [42]. Here we will focus on the work done following Dr. He's graduation, including instructions for electrical connections as well as results for the temperature tests with the STM scanner installed. Also described will be some modifications that need to be done in the future to improve the system's performance.

Finally Chapter 4 will summarize the results of the two projects as well as propose some future work, particularly what can be improved further and the directions of some possible extended projects in general.

1.6 Figures

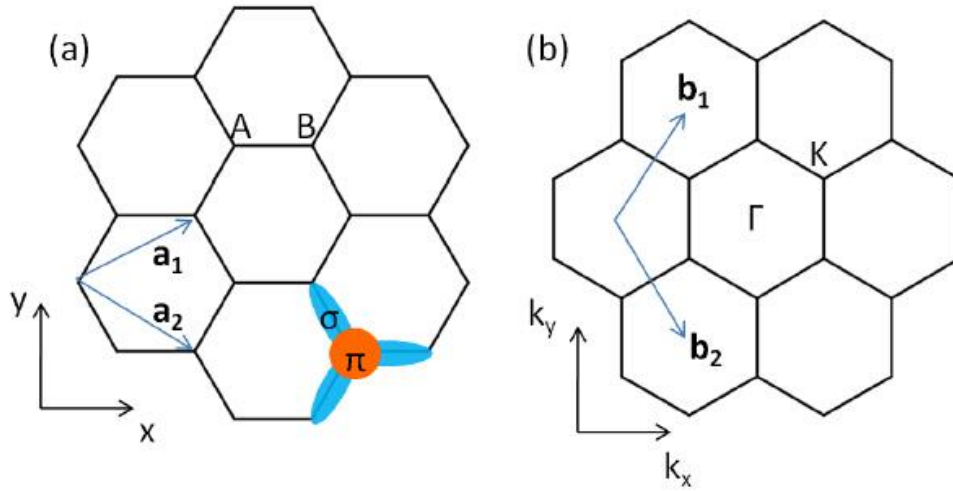


Figure 1.1 [12]. a) Real space honeycomb lattice structure of graphene: A and B represent two adjacent carbon atoms in a unit cell where each atom has three σ bonds in plane and one π bond perpendicular to the plane, and a_1 and a_2 are unit vectors that describe the unit cell. b) K-space representation of graphene with two unit vectors b_1 and b_2 .

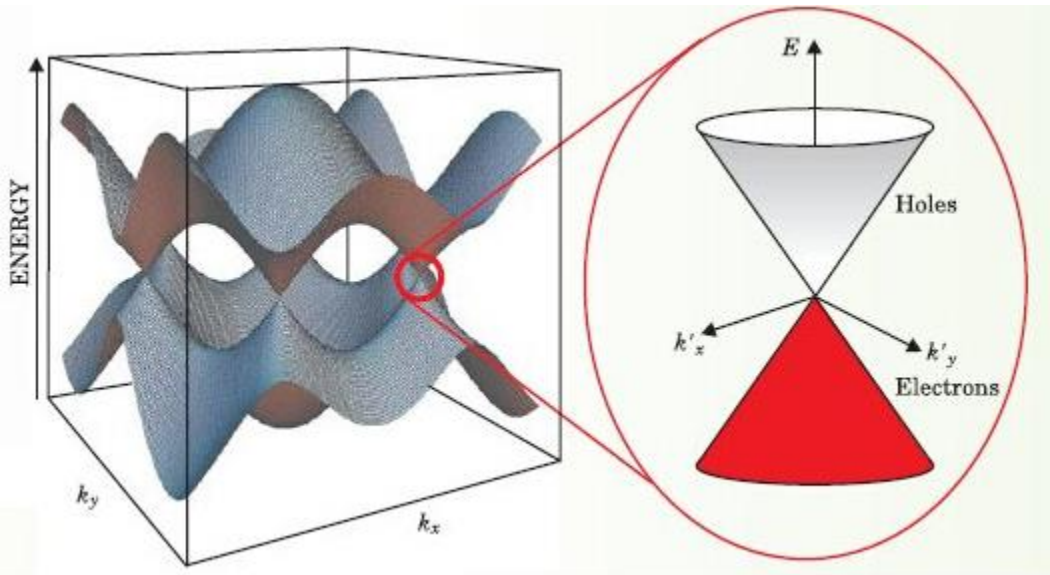


Figure 1.2 [21]. Three-dimensional representation of the dispersion relation of graphene: the conduction band and the valence band meet at one point, which is called the Dirac point, and energy changes linearly around the Dirac point in k-space.

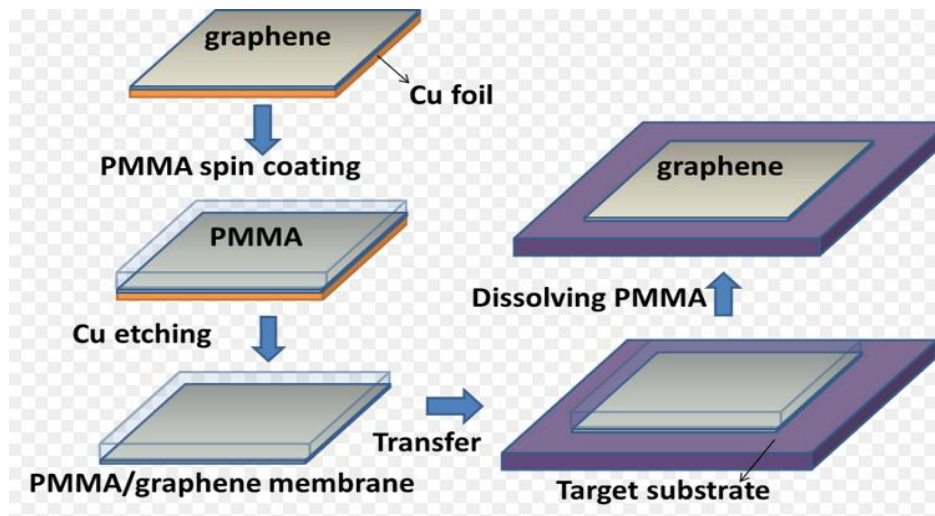


Figure 1.3 [26]. Conventional graphene wet transfer steps: first spin coat a layer of polymer such as PMMA, then etch the metal on which graphene grows, next transfer graphene with the polymer serving as support to the target substrate and finally dissolve the polymer, leaving graphene on substrate only.

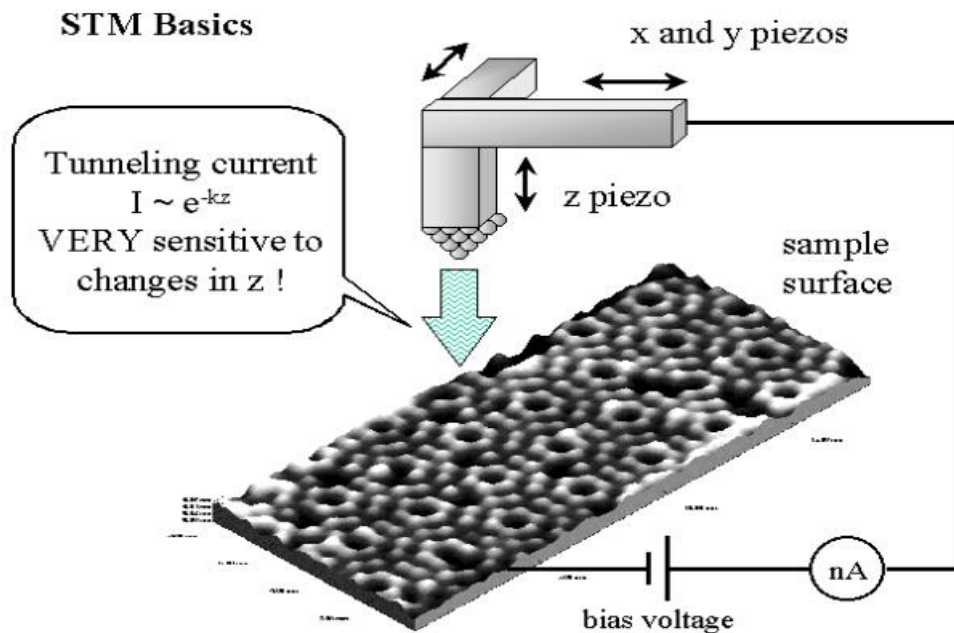


Figure 1.4 [37]. Illustration of STM basics: based on the concept of quantum tunneling, as a conducting STM tip is brought very close to a conducting surface with a bias applied between the two, current can tunnel through the vacuum barrier and is very sensitive to the tip-surface distance. Atomic information on topography of the surface (depends on the sharpness of the tip) can be obtained by maintaining a constant current while scanning across the surface with the control of x-y piezo-tubes.

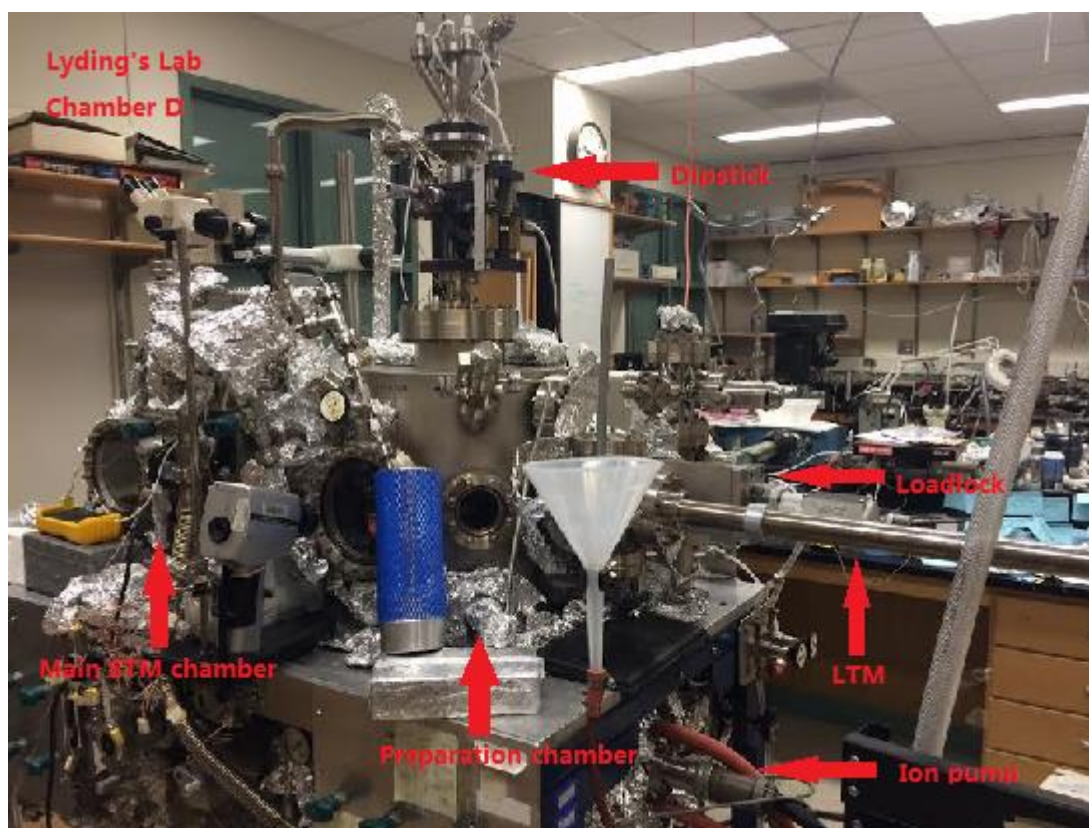


Figure 1.5. Photo of Chamber D in Lyding's lab. Samples are first loaded into the loadlock which is pumped by a turbo pump to 10^{-8} Torr and then transferred to the preparation (pumped by a ion pump to 10^{-11} Torr) via LTM. Samples needs to be degassed on the dipstick before finally transferring onto the scanner inside the main STM chamber where the actual scan takes place.

CHAPTER 2

LARGE-SCALE TRANSFER OF GRAPHENE ONTO CLEAN SURFACES IN ULTRA-HIGH VACUUM

2.1 Introduction and Motivation

As mentioned in Chapter 1, STM is a powerful tool for studying graphene-substrate interaction due to the fact that it achieves both atomic resolution topography and local electronic spectroscopy. However, for most STM studies on graphene, the graphene transfer process was performed in ambient conditions, which means there are chances of trapping residues [27] and water [29] between the graphene and the target substrate, causing a possible graphene doping or etching after a high temperature annealing. Since STM is designed to operate in an ultra-high vacuum (UHV) environment with its chamber base pressure ranging from low 10^{-10} to 10^{-11} Torr, one can get a very clean sample after appropriate sample preparation processes. For example Si is a highly reactive material which gets oxidized right away in air [45]. In an UHV environment, we can prepare clean silicon by heating it to a high temperature in the STM preparation chamber. And depending on the base pressure conditions, it will stay clean for hours to days. If graphene can be transferred in UHV onto a well-prepared clean substrate such as clean Si, not only will the residue issue be minimized but also many studies such as investigations of graphene as an oxidation resistance barrier for different substrates [45] [46] can be carried out.

The study of graphene deposited on clean Si is limited due to the difficulty of transferring large-scale of graphene in UHV. Some remaining questions left by previous studies [42] stated in Chapter 1 can be revealed with a large-scale graphene deposit. For example, if we want to find out whether the random distribution of the dangling bonds created beneath the graphene by H-

depassivation is due to electrons scattering in graphene or a large spot size of electron beam from the STM tip, we can do H-depassivation at the center of a large piece of graphene and see the distribution of the dangling bonds [42]. If the distribution is still random over a large area, it means the electrons indeed travel inside the graphene before tunneling through and if the distribution is concentrated over a small area, it means that we have a large electron beam from the tip and electrons are more likely to tunnel through the graphene directly.

Further investigations of graphene as an oxidation resistance barrier can be carried out by depositing large-scale graphene onto clean substrates such as clean Si in UHV. There are studies [45] [46] that have shown that graphene can efficiently prevent some metal surfaces from being oxidized in ambient conditions. However, one study has also claimed that the cracks in graphene would make the oxidation more severe [47]. With a large piece of graphene deposited onto a clean Si surface, we could take a close look at the graphene-substrate interaction in atomic scale under the STM: we can scan the graphene on clean Si first, let the sample be exposed to air and scan it again. By comparing the before and after images, the mechanism of how graphene prevents the surface from being oxidized can be further understood in detail.

2.2 Graphene Transfer Ex-situ Tests

Before doing the actual transfer in UHV, transferring graphene with three supporting materials was tried in ambient conditions. PET/silicone film, TRT and PDMS were chosen because they all have been reported as supporting materials for transferring graphene without using PMMA. They are also easy to handle and can be mounted onto an STM sample holder. We

would like to see the transferred graphene quality by using these stamping materials and therefore choose the best solution for the in-situ transfer.

2.2.1 Materials and Methods

The graphene used in this experiment was grown on 1 mil thick copper foils (99.9% pure copper, annealed for 90 minutes) by our group collaborator, Justin Koepke. With the prepared copper foils in the CVD furnace, growth was performed with 50 sccm of H_2 and 850 sccm of CH_4 flowing for 5 min at ~ 1000 °C. Then the furnace was cooled down to room temperature.

The substrate we used was a Si (111) wafer with 90 nm thickness of SiO_2 grown by plasma-enhanced chemical vapor deposition (PECVD). First, we degreased it with methanol, acetone, isopropanol alcohol (IPA) and de-ionized (DI) water. Then we cleaned it by dipping into a piranha solution (3:1 of H_2SO_4 : H_2O_2) for about 15 minutes, rinsed with water and dried with N_2 gas.

The solid PDMS was made by first mixing the PDMS base and curing agent with a ratio of 10:1 in a clean container, continuously stirring it for about 15 minutes to make sure that the curing agent is uniformly distributed. Then the mixture was kept in a bell-jar desiccator connected to a vacuum roughing pump for about 1 hour to pump out the trapped air bubbles. Lastly, the liquid mixture with the container was placed on a flat surface at room temperature overnight to fully cure. We chose to use the cured solid PDMS instead of pouring liquid PDMS onto graphene and then curing it because the latter gives better adhesion and is hard for graphene to release from the PDMS.

TRT was purchased from Nitto Denko America Corp (No. 3159, adhesion strength of ~ 3 N / mm, release temperature 120 °C) [48]. The PET/Silicone film was a piece of screen protector

film commercially made for the iPhone by SuperShieldz. The film is constructed in three layers: a scratch resistant surface polymer, a protective mask and a layer of silicone gel that creates a vacuum to securely “cling” to any surface [49].

For the pre-transfer process, graphene grown on Cu was cut into 5 mm² pieces and flattened with two piranha-cleaned glass slides. PDMS, TRT and PET films were cut into 1 cm² pieces. Only PDMS requires degrease cleaning with methanol, acetone and IPA because the other two have release liners that need to be peeled off right before the transfer. The first step is to press graphene onto these supporting materials. A large and uniform force is required to ensure a good contact between graphene and those materials so we used a bench vise to press them together tightly for 30 minutes to 1 hour. Next we etch away the exposed side of the graphene by a reactive ion etching process. And then the copper etch: letting the sample float on the FeCl₃ etchant solution with the graphene side facing downward for more than 5 hours can completely remove the copper. We have also tried another copper etching solution, ammonium persulfate: it tends to leave fewer residues, but it generates many bubbles during etching and damages our graphene, so we stayed with the FeCl₃ solution. After copper is removed, the graphene/supporting material sample is moved to a DI water bath for 15 minutes, then a 10% HCL solution for 10-15 minutes followed by another DI water bath for 15 minutes to remove the etchant residue. After letting the sample dry in air or on a hotplate at a temperature of < 50 °C for more than 30 minutes, the graphene sample is ready for the transfer.

Graphene on TRT was pressed against the SiO₂/Si chip tightly for over 30 minutes using the vise to ensure a good contact between graphene and the SiO₂ surface. Then we removed the Si/graphene/TRT stack onto a hotplate (temperature set to 130 °C, 10 °C above the releasing temperature of the TRT). Graphene is released from the TRT while adding heat for about 30

seconds. No force is required during the heating process; otherwise, the TRT will rebound to graphene and leave a lot of residue.

For graphene transferred by PDMS, we also pressed it against the Si chip tightly for over 2 hours using the vise to ensure a good contact. Then with the PDMS/graphene/Si sample stack, we carefully peeled off the PDMS, leaving graphene stamped on Si.

Graphene transferring from the PET film onto Si does not require great force. Simply put the PET with graphene onto the Si chip and press lightly using one hand for about 20 seconds. Due to the larger adsorption force between graphene and the SiO₂ surface [50], graphene will adhere to the SiO₂ after peeling off the PET film. Heating the Si chip up to 40 °C - 50 °C during the transfer process can improve the degree of contact between graphene and the SiO₂ surface and result in a better transfer.

2.2.2 Results and Discussion

The resulting transferred graphene on SiO₂/Si substrate by TRT, PDMS and PET film are characterized by optical microscopy and scanning electron microscopy (SEM). All SEM images were taken using a field-emission environmental SEM with an ultra-high definition mode at 5kV. We tried to maintain similar brightness and contrast values so that the images can be easily compared. Figure 2.1 shows the optical images of graphene transferred by a) TRT, b) PDMS and c) PET. Both TRT and PET gave a better coverage of graphene macroscopically compared to PDMS. PDMS seems to stick with graphene better, so even with a larger force and longer time during the stamping process, the overall coverage is not as good. Besides transfer yield, we can see that both TRT and PDMS leave some residue on the SiO₂ surface, whereas the residue for PET is not visible under optical microscope. The coverage and residue issues make the PDMS-

based transfer less appealing. It is worth mentioning that we have also tried using another type of TRT which has weaker adhesion strength of 1 N / mm [48]. The resulting graphene coverage turned out to be worse. So TRT with stronger adhesion strength is better for graphene transfer.

Since the composition of the TRT is unknown, in order to get rid of the residue left by TRT, we put one TRT transferred graphene sample in acetone overnight. Figure 2.2 shows the SEM images of the TRT residue before and after acetone treatment: a) shows the area where residue is on SiO₂ and b) shows the area where residue is on graphene. We can see that TRT residue can be somewhat dissolved by acetone but not completely so. We further put the sample onto a hotplate at 450 °C for 1 hour. Figure 2.3 a) shows the SEM images of TRT residue on Si before and after annealing and b) shows the images of TRT residue on graphene before and after annealing. Graphene can be clearly seen from the zoomed-in image, so it seems that the most TRT residue has evaporated during the annealing process. This means we can get rid of the residue by degassing the sample. However the UHV compatibility of the TRT is unknown before its rate of outgas is determined [51].

To further evaluate the quality of transferred graphene, we compared SEM images of graphene transferred by TRT (Figure 2.4a), PDMS (Figure 2.4b) and PET (Figure 2.4c). We observe poor continuity for graphene transferred by TRT compared to the other two methods. By comparing the resulting graphene transferred by the three methods (as concluded in Table 2.1), and considering the overall high transfer yield, less residue, good continuity and tractable transfer process, we decided to use PET film for the in-situ transfer.

2.3 Graphene Transfer in UHV

The in-situ graphene transfer from PET film to a Si sample was performed in the STM preparation chamber with a base pressure of $\sim 3 \times 10^{-10}$ Torr.

2.3.1 Sample Preparation and Transfer Methodology

A boron-doped Si (100) wafer was first cleaned by performing a RCA process [52] and piranha solution [53], then was cut into the STM sample size and mounted onto a sample holder. After degassing the sample on the dipstick in the preparation chamber overnight by running a current across the sample, we flashed the Si sample at 1250 °C for 30 seconds while maintaining the chamber pressure below 5×10^{-9} Torr to get rid of the native oxide. Once the flashing was finished, we let the sample cool down to room temperature. Then it was transferred to the STM main chamber for scanning and to check its cleanliness. We scanned the surface at -2.0 V and 0.5 nA with a scan angle of 45° relative to the (100) direction. Figure 2.5 shows representative STM topographic and current images of the flashed Si sample we prepared: clear Si (100) surface 2×1 reconstruction dimer rows [54] and steps with 90° rotation of the dimer rows indicate that the Si surface is clean and ready for the transfer.

The graphene on PET film was prepared ex-situ as described in section 2.2.1. The DCT applicator was made by gluing the graphene/PET film onto a modified fiberglass piece using an UHV-compatible epoxy and attaching it to a sample holder (shown in Figure 2.6). Then it was loaded onto the LTM in the preparation chamber.

The in-situ transfer is realized by securing the flashed Si sample on the dipstick and bringing the graphene/PET towards it using the LTM (as shown in Figure 2.7). Transferring graphene without heating the Si sample was initially tried. We pushed the LTM until the

graphene was in contact with the Si surface and held it for ~30 seconds. The softness of the fiber glass will dampen the force between graphene and Si to ensure a full contact and avoid cracking the sample. After holding for about 20 seconds, we slowly pulled the LTM away from the Si sample to separate the PET film from the Si sample. We noticed that the PET film tends to stick with the Si surface once they are in contact. To prevent the sample holder for the PET film from sliding out of the LTM, we twisted the LTM a little bit in order to separate the PET film from the Si sample.

We also tried a transfer with the Si sample being heated by the dipstick at 40 °C. However, we realized a chamber pressure jump up to 10^{-5} Torr during the transfer, which indicates a high rate of outgassing. Later we found that it was the epoxy that causes the overpressure. We tested the epoxy on a hotplate at 40 °C in ambient condition and found that it would melt completely into liquid within 3 minutes.

2.3.2 Characterizations and Discussion

The Si sample with graphene transferred in situ does not show obvious color contrast optically (as shown in Figure 2.8d), so overall coverage wasn't obvious right away unless we took the sample out and checked with SEM. Characterizing the sample with STM was the first step. Unfortunately no graphene or Si dimer rows were seen using STM. Instead, a strip-patterned feature on the surface with the strip width of 1.5 - 2 nm and height of ~0.1 nm was observed (as shown in Figure 2.9a). This could be the silicone gel residues from the PET film. An interesting fact was that the strips also rotate at 90° at a step and seem to lay along with the direction of the silicon dimer rows (Figure 2.9b). Whether the superposition of the orientation of these strips and the dimer rows is a coincidence or the residue tends to bond with the dangling bonds of the Si substrates needs to be investigated with more scans in the near future.

In order to confirm the success of the transfer, the sample was taken out of the STM chamber and inspected under SEM to get the overall transfer yield. Figure 2.8 (a,b) shows the SEM images of the first attempted in-situ transferred graphene on Si sample with different magnification scales. The transfer yield was not as good as the ex-situ transferred case. Two large pieces of graphene were found, one with a size of $\sim 2 \text{ mm}^2$ and the other one $\sim 1 \text{ mm}^2$. Zoomed-in image (Figure 2.8c) shows that the continuity of transferred graphene is also bad compared to the results from the ex-situ case. Since the thickness of the native oxide layer is less than 1 nm [45] and both graphene and Si substrate are conductive, with the high energy electron beam of 5 keV, the definition of the SEM images for in-situ transferred graphene on Si is not as good as the one for ex-situ graphene on SiO_2 . We could not get a clear zoomed-in image to take a closer look at the graphene.

To further evaluate the success of the transfer, we used a Bruker Dimension III Atomic Force Microscope (AFM) with a Si tip (in tapping mode) to characterize the topography of the sample. Figure 2.10a is the AFM image of graphene transferred onto Si. With a higher resolution provided by the AFM, we recognized some graphene pieces which have a much smaller surface roughness compared to the substrate. The line analysis of AFM image (shown in Figure 2.10b) gives the height profile of 0.5 nm step height, corresponding to a single layer of graphene [55]. The AFM images also confirm the poor continuity of transferred graphene with the size of graphene in the micrometer scale which is consistent with the SEM image. One possible cause could be graphene was torn by the action of LTM twisting when we were trying to separate the PET film from Si.

2.4 Conclusion and Future Work

In conclusion, we were able to transfer CVD-grown graphene using PET film as a support onto a clean Si sample in an UHV STM chamber via modified DCT method. The low surface tension of the PET film makes graphene easy to release. Ex-situ tests show that the PET film gives the best transfer yield and continuity compared to TRT and PDMS and makes in-situ transfer feasible. The transferred graphene was imaged by SEM and AFM. Without heating the Si sample during transfer, we transferred a total area of $\sim 3 \text{ mm}^2$ out of $\sim 15 \text{ mm}^2$ of graphene. AFM reveals the size of each individual graphene piece to be on the micrometer scale, and this is a big improvement compared to the nanometer-scale transfer done by Ritter [39].

Ex-situ tests as well as a study [56] have shown that transfer yield can be improved by transferring onto a hot substrate. We are going to find a different epoxy that is UHV compatible when heated and try the in-situ transfer onto a heated Si next time. Also we need to modify the sample holder in order to prevent it from sliding out of the LTM when detaching the PET film from Si. More STM scans are needed in order to find out if re-degassing the sample can make the silicone residue left on the Si surface evaporate.

2.5 Figures

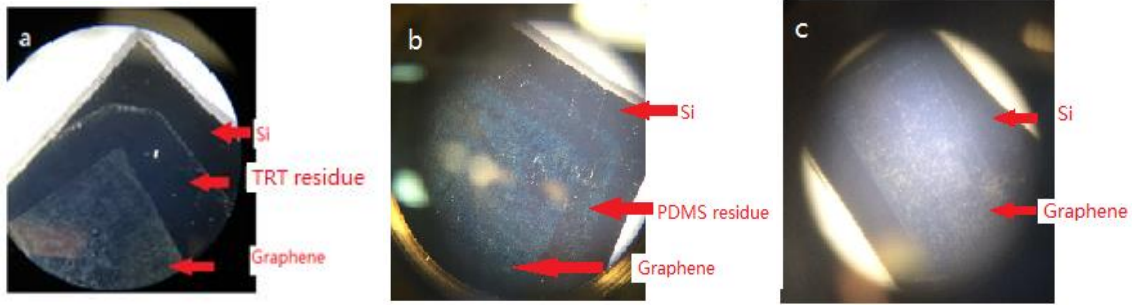


Figure 2.1. Optical microscope images of ex-situ transferred graphene on SiO_2/Si by a) TRT, b) PDMS and c) PET/silicone. The size of the transferred graphene is about 1 cm^2 . Both TRT and PET gave a good coverage of graphene macroscopically. However, the residue from the TRT is much more obvious than PDMS and PET/silicon. And compared with the other two materials, PDMS seemed to stick better with graphene. It requires a much longer time (several hours) and greater force to be applied during releasing, and its transfer yield is not as good and it also left some residue.

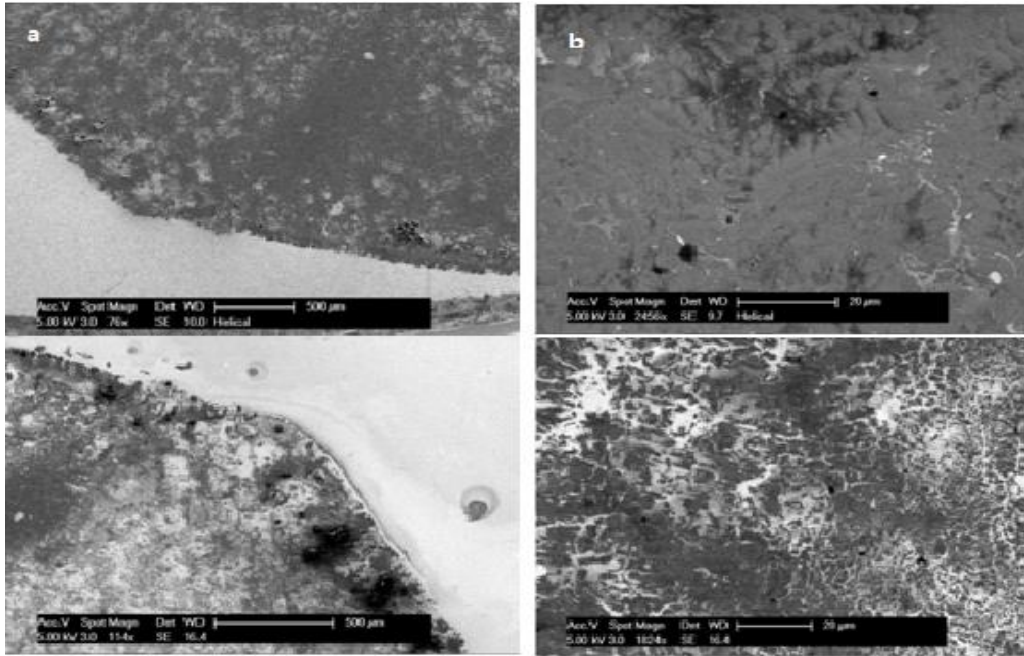


Figure 2.2. SEM images of TRT residue: a) TRT residue on Si before (top) and after (bottom) been treated with acetone. Scale bar is $500 \mu\text{m}$. b) TRT residue on graphene before (top) and after (bottom) being treated with acetone. Scale bar is $20 \mu\text{m}$. By comparing the before and after images, we can see that acetone can dissolve some but not all of the residue.

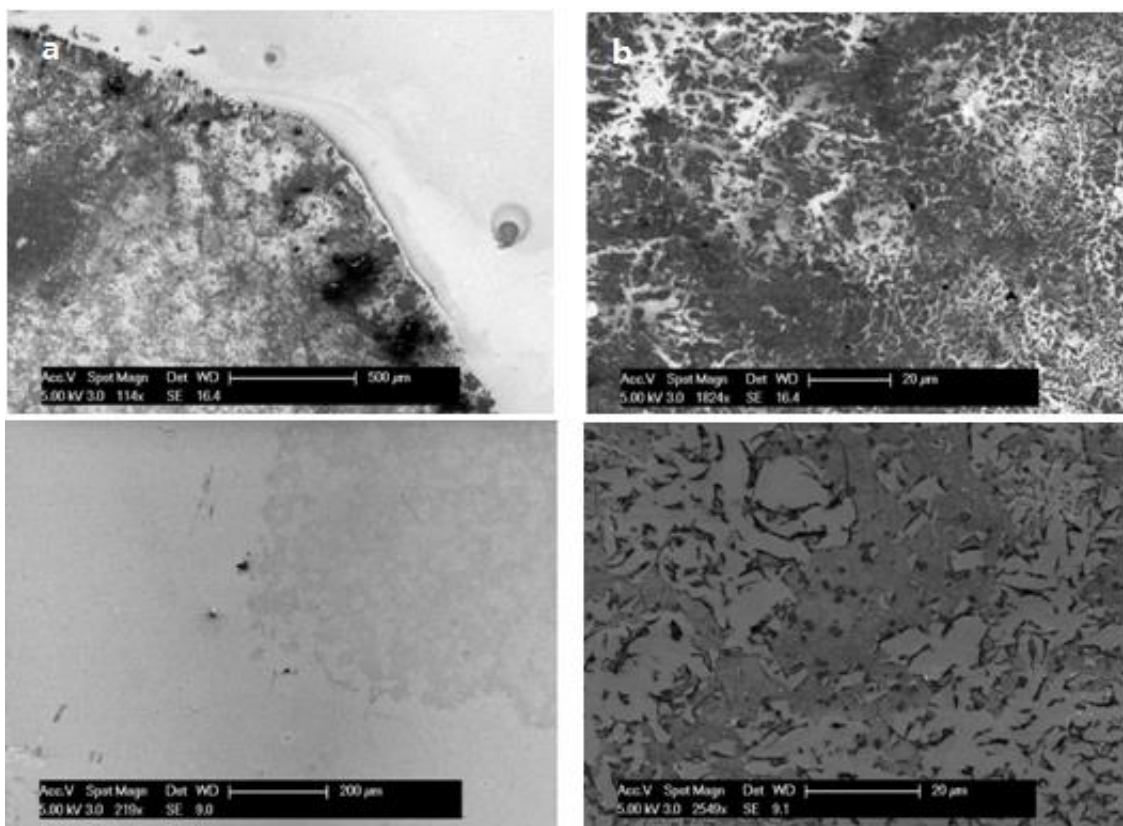


Figure 2.3. SEM images of TRT residue: a) TRT residue on Si before (top) and after (bottom) annealing on a hot plate at 450 °C for 1 hour. Scale bar is 500 μm and 200 μm . b) TRT residue on Graphene before (top) and after (bottom) annealing. Scale bars are 20 μm . By comparing the before and after images, we can see that the TRT residue was efficiently evaporated during the annealing process.

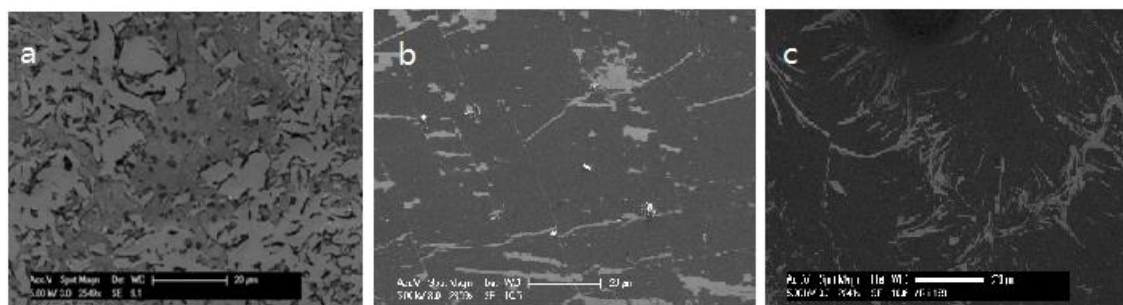


Figure 2.4. Zoomed-in SEM images of graphene transferred by a) TRT after high temperature annealing, b) PDMS without any post treatment and c) PET/silicone film without any post treatment. The continuity of graphene transferred by TRT is poor whereas PDMS and PET transferred graphene gave fairly good continuity. The breaks in graphene transferred by TRT could be caused by the etching of oxygen gas during the high temperature annealing process and can be avoided during a UHV degas process. Scale bar are 20 μm for all images.

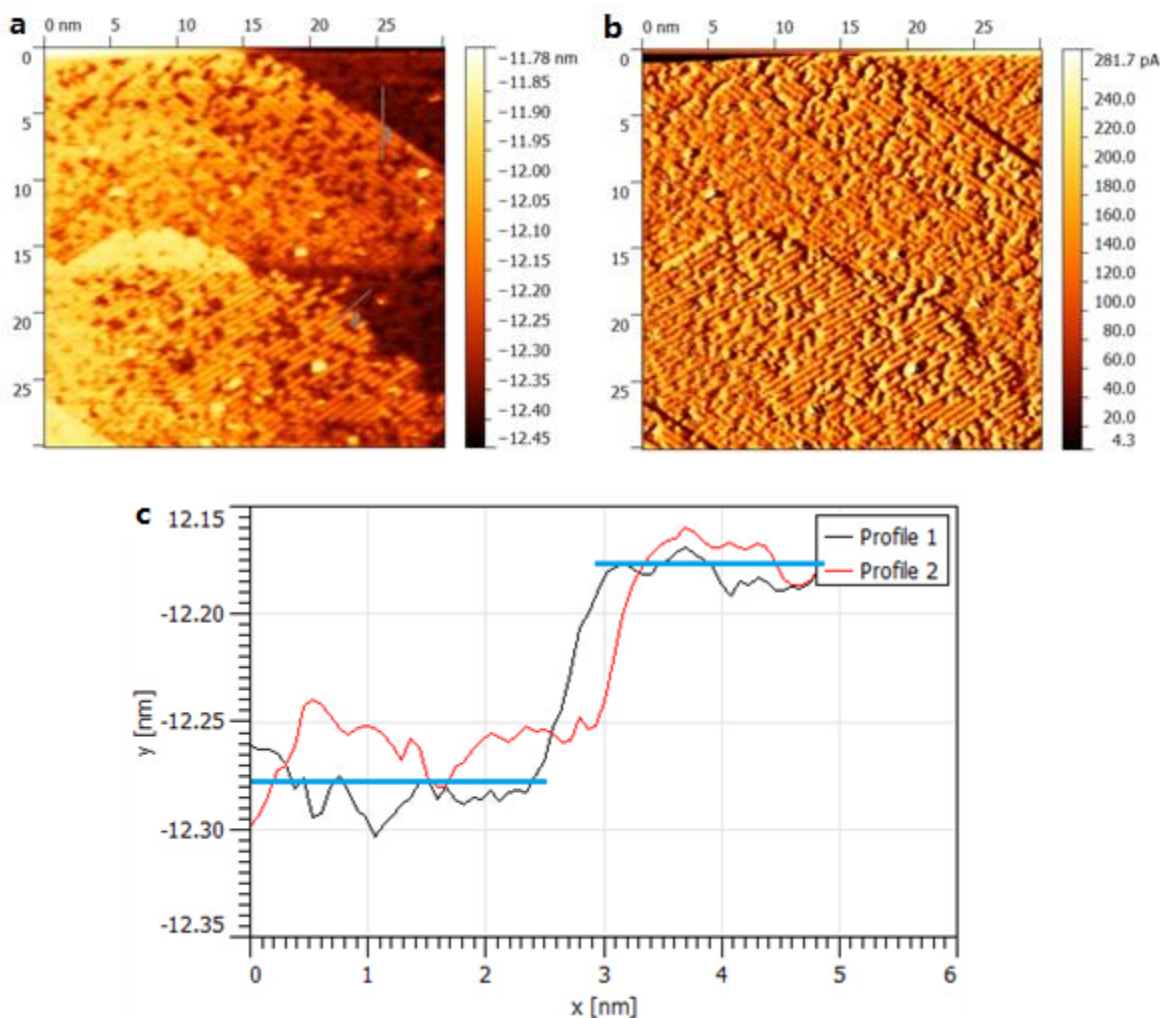


Figure 2.5. STM images of clean Si surface after flashing: a) topographic and b) corresponding current images, scan area is 900 nm^2 , scan conditions are: -2 V , 0.5 nA . Si dimer rows can be clearly seen with vacancies and few contaminants. Orientation of dimer rows rotates 90° between steps. c) The height profiles of the two steps on Si surface in a); steps height averages 0.1 nm , which indicates a very flat surface.

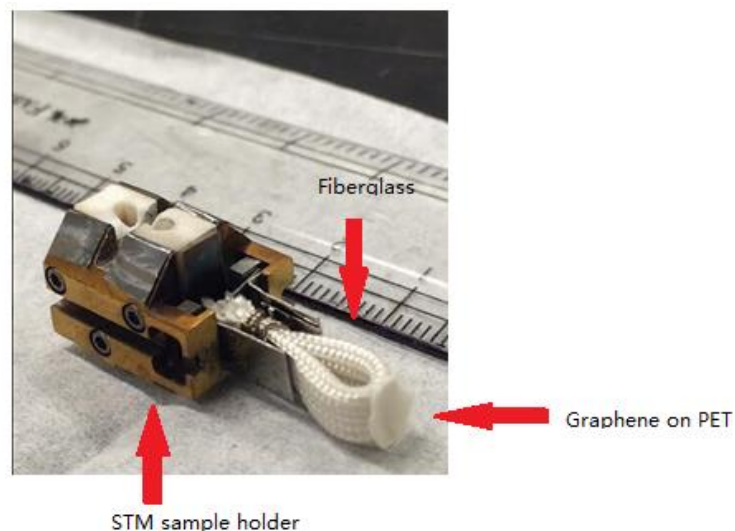


Figure 2.6. Picture of DCT applicator for in-situ transfer. PET film was glued onto the fiberglass which is mounted onto a STM sample holder. Fiberglass was used to dampen the force during stamping to ensure a good contact between the PET film and the target substrate surface. Both the epoxy and the fiberglass are UHV-compatible.

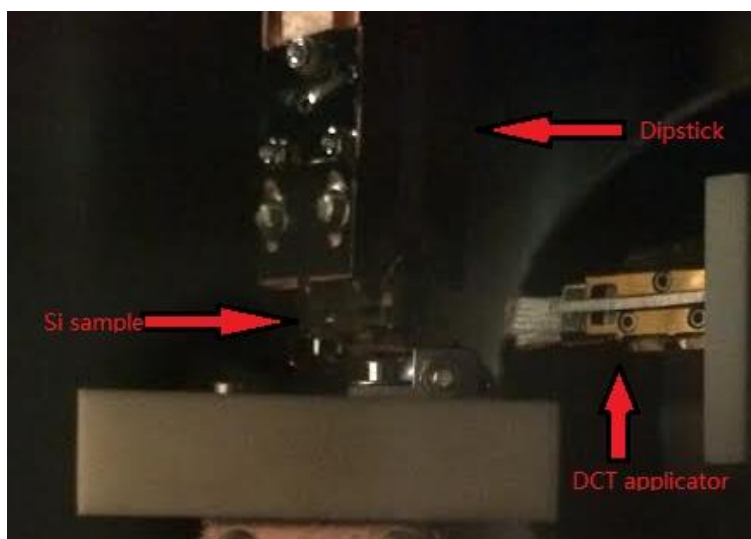


Figure 2.7. Picture of in-situ transfer inside the STM preparation chamber. A clean Si sample was loaded on the dipstick facing the DCT applicator which is on the LTM. We pushed the LTM towards the dipstick to let the PET film come into contact with the Si sample, held for 30 seconds to separate graphene from the PET film and then pulled the LTM away to complete the transfer.

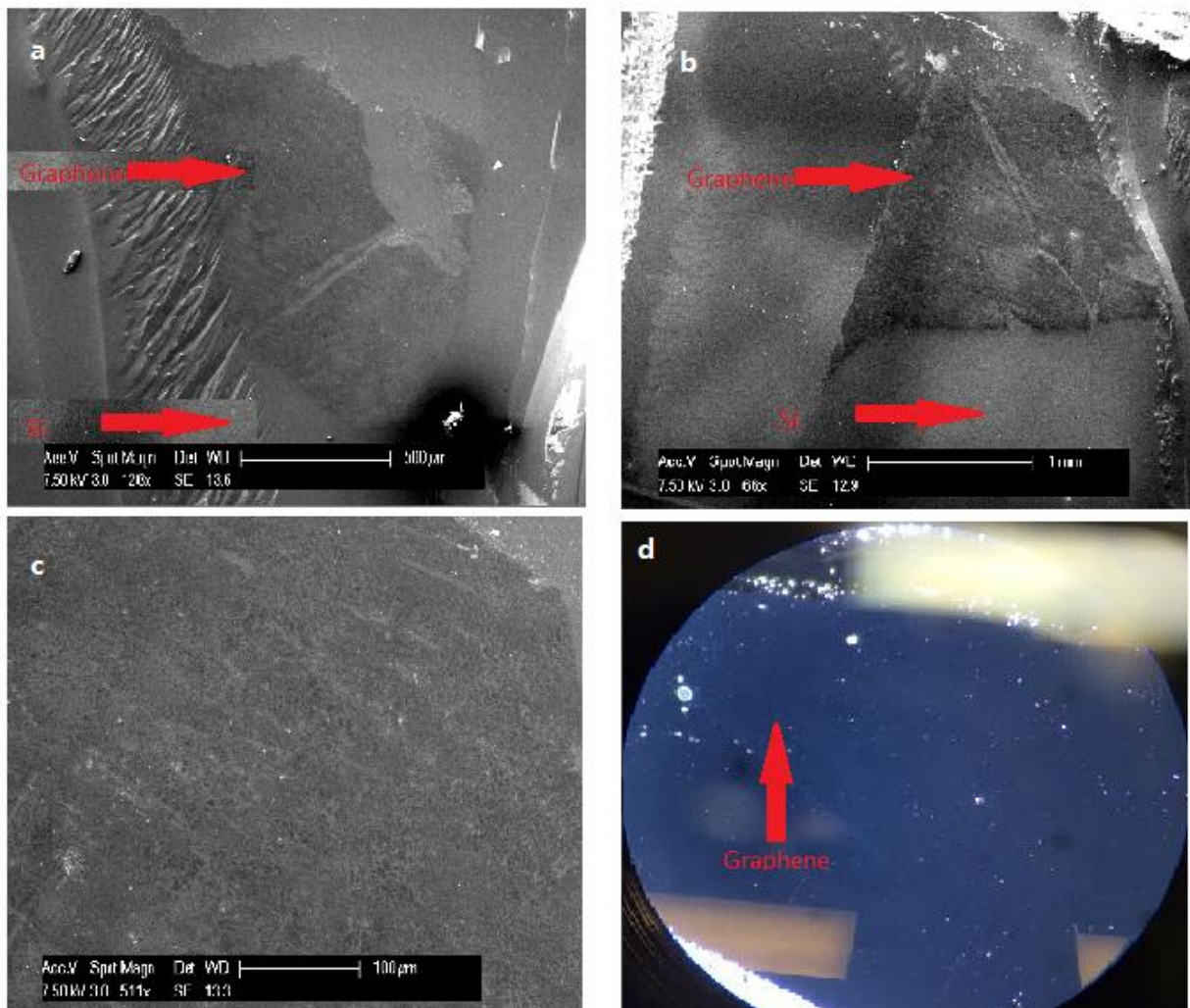


Figure 2.8. SEM images of in-situ graphene transferred on Si. a) and b): Two graphene pieces found under SEM with sizes of $\sim 1 \text{ mm}^2$ and $\sim 2 \text{ mm}^2$ respectively. Scale bars are 500 μm and 1mm. c) Zoomed-in image which indicates that the transferred graphene does not have good continuity; breaks were seen everywhere and could be caused by the twisting of the LTM when separating the PET from the Si sample. Scale bar is 100 μm . d) Optical microscope image: graphene/Si contract is not clear and graphene can be barely recognized.

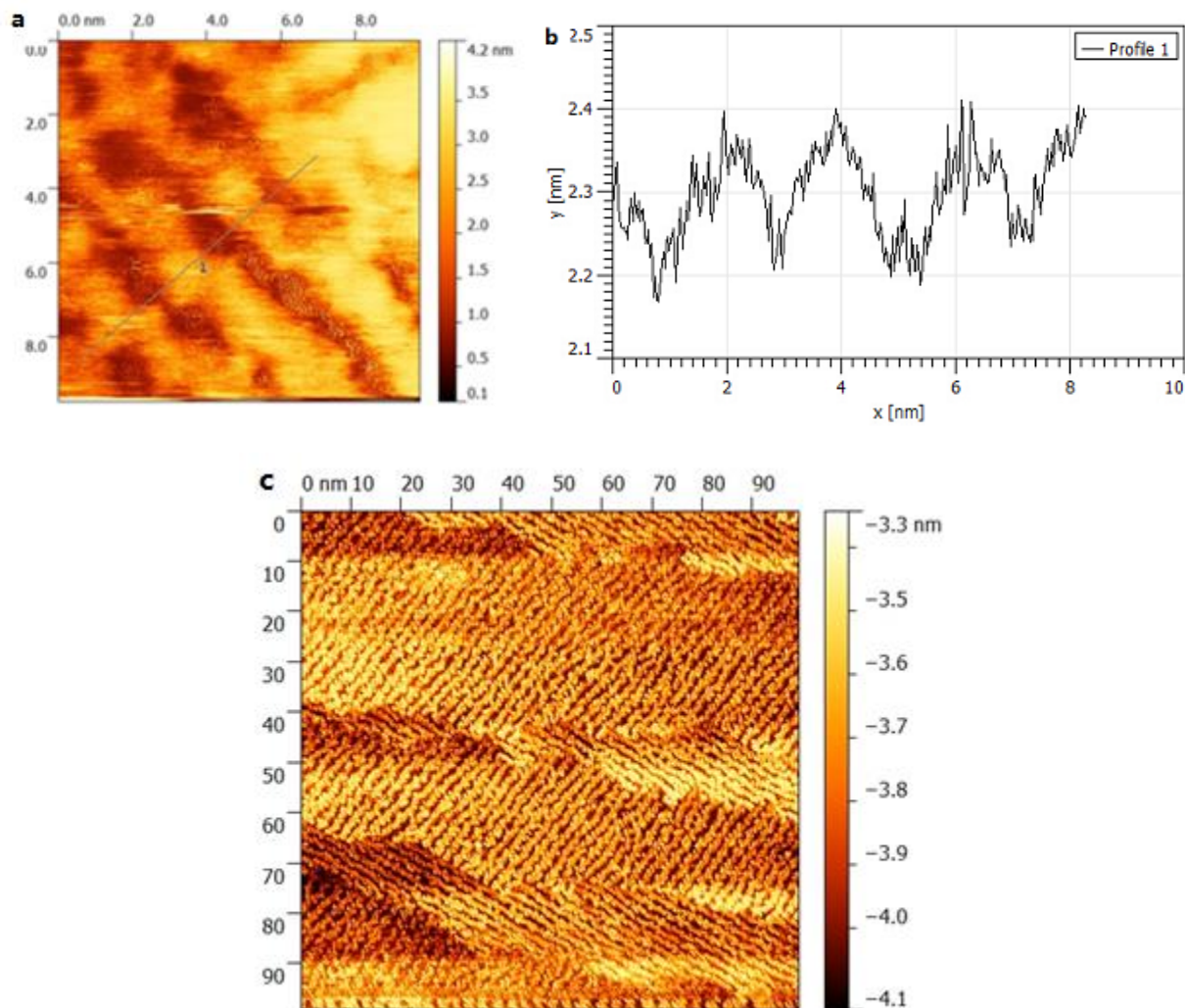


Figure 2.9. STM topographic images of Si surface after transferring graphene. a) and b) show that strip patterns with 2 nm width and 0.2 nm height were observed, scan area is 100 nm². c) Larger image shows that those strips were reoriented in 90° increments in adjacent steps. No graphene was found under STM, scan area is 10000 nm². These strips could be silicone residues from the PET film and the reason that they lay along the direction of the Si dimer row needs to be determined with more scans.

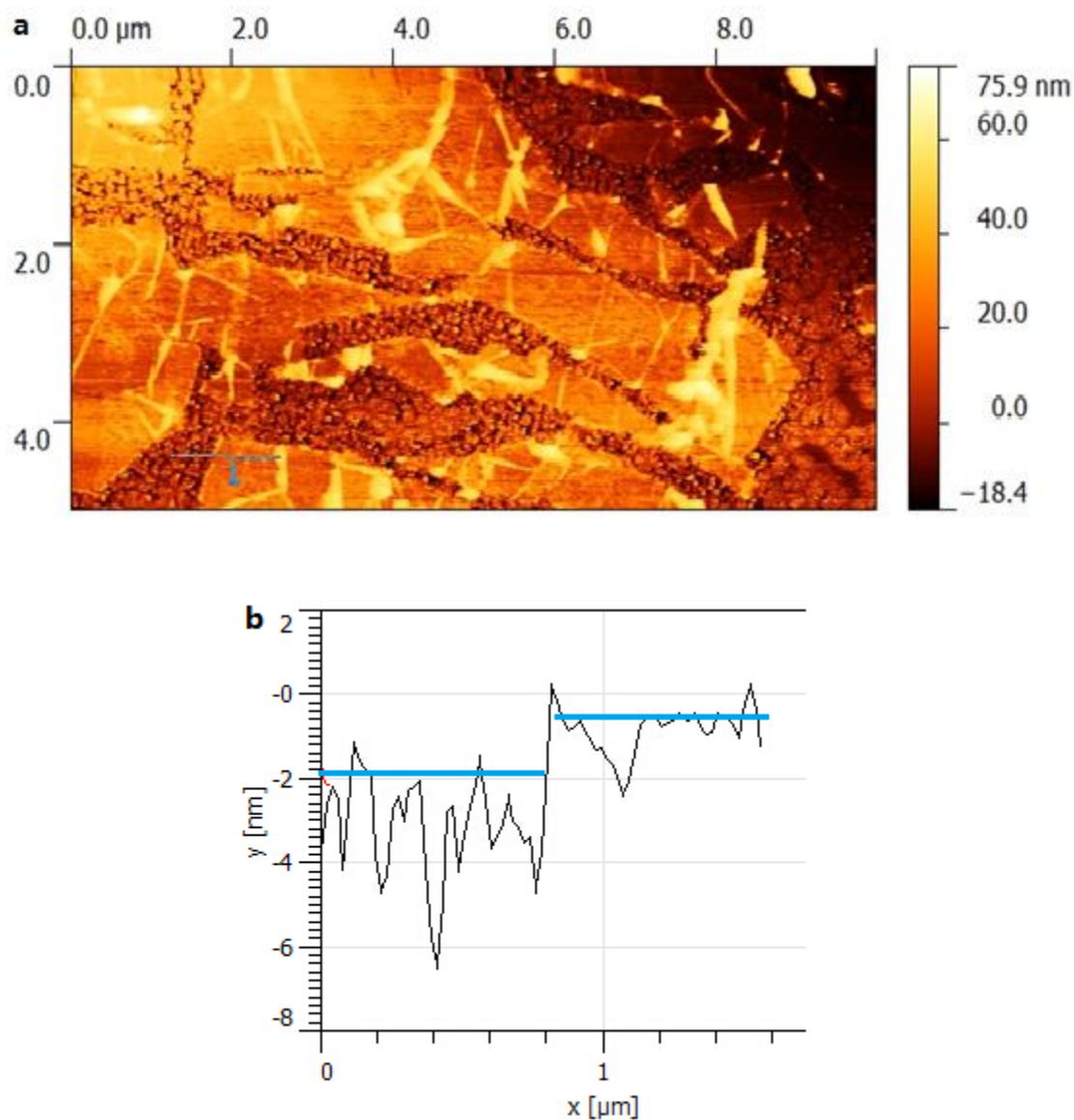


Figure 2.10. AFM image of in-situ graphene transfer on Si. a) The success of transfer is confirmed under AFM where graphene flakes were clearly seen. b) Height profile shows that the height of graphene is ~ 0.5 nm, which indicates a monolayer of graphene.

2.6 Table

Table 2.1. Conclusion of graphene transfer ex-situ by TRT, PDMS and PET film. Compared to the other two methods, graphene transferred by PET film gave the largest transfer yield, best continuity, least residue and least release force/time. Therefore it is the best candidate for in-situ transfer.

Graphene Transfer	Transfer Yield	Continuity	Residue Left	Release Force Required	Release Time
TRT	Large >90%	Poor	Lot	Large (by vise)	0.5 hour
PDMS	Low <50%	Good	Not much	Large (by vise)	2 hours
PET/Silicone	Large >90%	Good	Very little	Small (by hand)	20 seconds

CHAPTER 3

DESIGN OF A LOW TEMPERATURE ULTRA-HIGH VACUUM SCANNING TUNNELING MICROSCOPE

3.1 Background and Motivation

Scanning with a sharper tip can undoubtedly improve the real-space resolution of the images obtained by STM since the radius curvature of the tip determines the size of the tunneling electron beam. However, even with a very sharp tip, electrical noise as well as the induced movement of absorbed atoms and molecules between the tip and the surface are inevitable and therefore affect the stability of the scan. Researchers have found that operation at cryogenic temperatures can reduce the thermal drift as well as freeze those absorbates [57]. Therefore resolution is improved and makes manipulation of atoms and molecules by the tip much easier. Furthermore, low temperature STM enables the study of physical phenomena such as superconducting materials [58] and interactions between molecules/atoms [59] that can only be observable at a low temperature.

There are various low temperature (LT) STMs that have been built [59] [60]. In order to reach temperatures below 10 K, liquid helium is the required cryogen. However, maintaining the low temperature during scans requires interruption of the experiment to replenish the liquid helium, precluding the automated performance of long scanning and spectroscopy sequences. Furthermore, costs have risen sharply for liquid helium, thus adding an additional barrier to these experiments.

3.2 Design Concept and Previous Work

We decided to implement a novel design of the cooling mechanism, which is to use a closed-cycle helium-based refrigerator to cool the system instead of using dewars of liquid helium. The refrigerator (as shown in Figure 3.1) we bought includes a compressor that provides helium gas to an expander and is able to cool it at 4 K for a total of 12000 hours without replenishing helium gas. Since the expander needs to be placed in an upward position, we had no choice but to place it at the back of the STM chamber. The expander has two stages with the first stage being cooled to 70 K and the second stage at 4 K. In order to keep the scanner cool, we designed a two-box configuration with the outer box connected to the first stage of the expander by a shield and the inner box connected to the second stage by a solid rod. The STM scanner is therefore sitting inside the inner box for cooling and suspended by a spring from the top of the chamber while scanning. A picture and a diagram of our whole system design are shown in Figure 3.2.

The STM scanner needs to be suspended during scanning to isolate the vibration from the outside. It is realized by attaching it to heavy weight which is hung by a spring from the top of the chamber (as shown in Figure 3.3). The position of the spring is adjustable via an x-y-z manipulator. The easiest way of installing is to put the scanner in the box first and screw the thinner rod into the Teflon piece that is attached to the scanner. Then screw the thicker rod into the thinner rod while holding the scanner. And finally, screw the thicker rod into the copper weight while holding the scanner.

Minimizing the thermal leakage and heat radiation were kept in mind along our way of design: a two-box configuration helps reduce the heat radiation from the scanner; Teflon spacers which have smaller thermal conductivity [61] were used to the largest possible extent to replace

metal pieces in order to reduce thermal leakage from the boxes to the chamber and scanner to the spring; indium foils and braided copper were added between joints to help cooling along the way from the expander to the boxes.

For more details about the previous designed parts including the boxes, coldfinger, shields and the suspension mechanism as well as the maintenance and operation of the system, one can refer to a dissertation [42] written by Dr. He and Ximeng Liu's undergraduate Senior Thesis [44].

3.3 Electrical Connections

Since the scanner is inside the two boxes, two feedthroughs embedded on each box were designed for electrical wires to pass through from the scanner to the cable connector outside the boxes. The feedthroughs were made of Shapal-M [62] which serves as both a good electrical insulator and a good thermal conductor and were imbedded on the side of the two boxes. Each feedthrough has 20 little holes that were plugged with little screws. And the outside screw ends of the inner-box were connected to the inside screw ends of the outer-box accordingly by soldering them with Teflon coated stainless steel wires. Temperature simulations of our system by COMSOL Multiphysics showed that an increase of the diameter of the wire from 0.01 inch to 0.02 inch would cause a temperature rise from 14.19 K to 16.8 K. So we chose the thinnest wires we could get. In order to make the installation and un-installation easier, we soldered one little gold pin on every screw's head. With another gold pin soldered with the wire that is connected to the scanner or the temperature, we can connect/disconnect them by simply plugging/unplugging one gold pin from the other. Extra care needs to be taken since those thin wires are fragile and

easy to detach from the soldering pins. Figure 3.4 provides a drawing and an actual picture of the feedthrough for better understanding. There are a total 15 wires that need to be connected inside the box: eight for the two temperature sensors; two for the scanner rails and five for the piezo-tubes. An additional current probe wire goes through the holes on top of the boxes since it requires a coaxial wire.

3.4 Temperature Test Results and Discussion

With the STM scanner assembled and the suspension installed, we tested the temperature by installing two temperature sensors: one attached to the inner box and the other one attached to the scanner. Results (shown in Figure 3.5) showed that the temperature of the inner box reached ~ 18 K and scanner reached ~ 28 K with it sitting on the box after 26 hours of cooling. It is worth mentioning that the temperature of the scanner was still dropping at a very slow rate after 26 hours. The thermal leakage from the suspension could cause the temperature difference and a bad contact between the scanner and the inner-box made the scanner's temperature drop slowly.

In order to see how much the suspension can affect the temperature of the scanner, we ran another test by lifting the scanner up during cooling. The temperature rose from 36 K to 55 K within 2 hours and finally stabilized at ~ 58 K after 20 hours (see Figure 3.6). It seems like the leakage by the suspension is the major factor for the higher temperature of the scanner and this result is consistent with our previous simulation run by COMSOL [42].

In order to reach our desired temperature (< 10 K), several modifications can be made. We can shrink the area of the Teflon block which is between the scanner and the suspension rod or we can add some fiberglass which has a thermal conductivity of 0.04 W/mK (1/6 of Teflon)

[61] to reduce thermal leakage since the amount of heat flow per unit time is proportional to the contact area and thermal conductivity [63].

3.5 Conclusion and Future Work

In conclusion, we designed a LT-UHV-STM that is capable of scanning at ~30 K. A new cooling mechanism that uses a refrigerator to cool the system was implemented to make the operation easy. With the scanner and the suspension installed and all of the electrical connection tested, the system is ready for doing scans under turbo vacuum conditions ($\sim 10^{-8}$ Torr).

In addition to further reducing the thermal leakage, future work includes: designing a way to open/close the side windows as well as the front doors of the boxes, and designing a locking mechanism for the STM holder during sample loading/unloading.

3.6 Figures

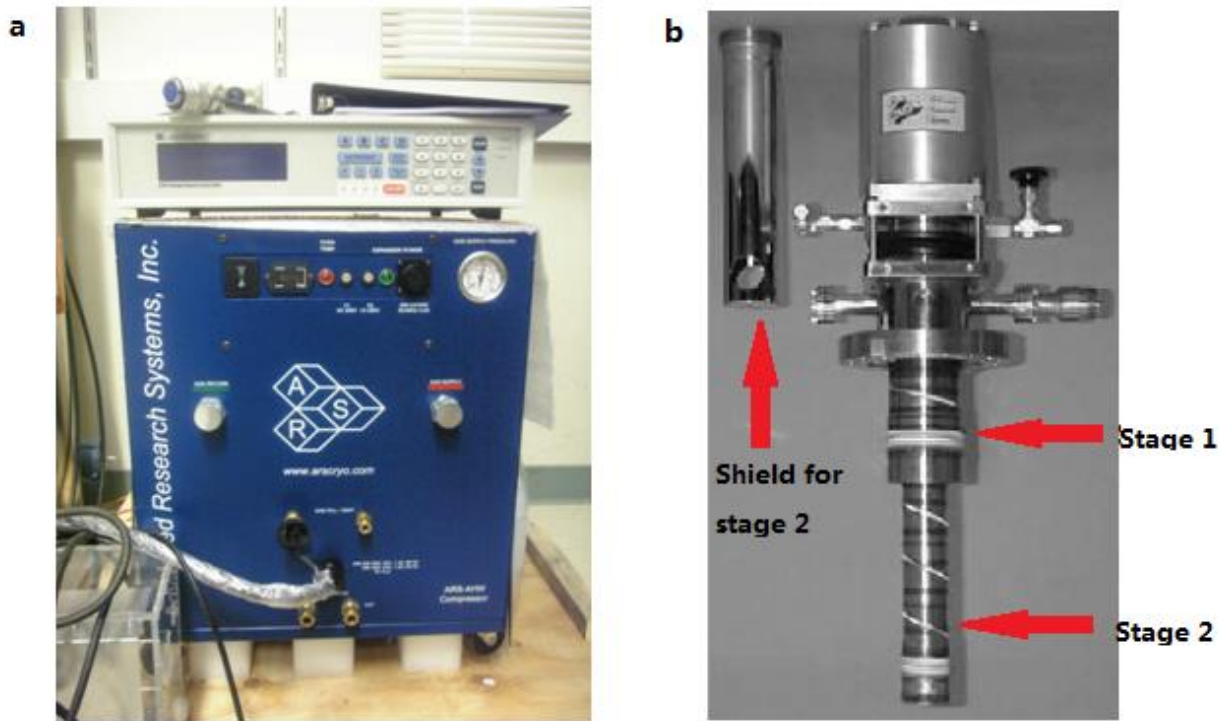


Figure 3.1. Refrigerator brought from Advanced Research Systems (ARS), Inc. a) Photo of the compressor. b) Photo of the expander from ARS with stage 1 reaching 70 K and stage 2 reaching 4 K during operation.

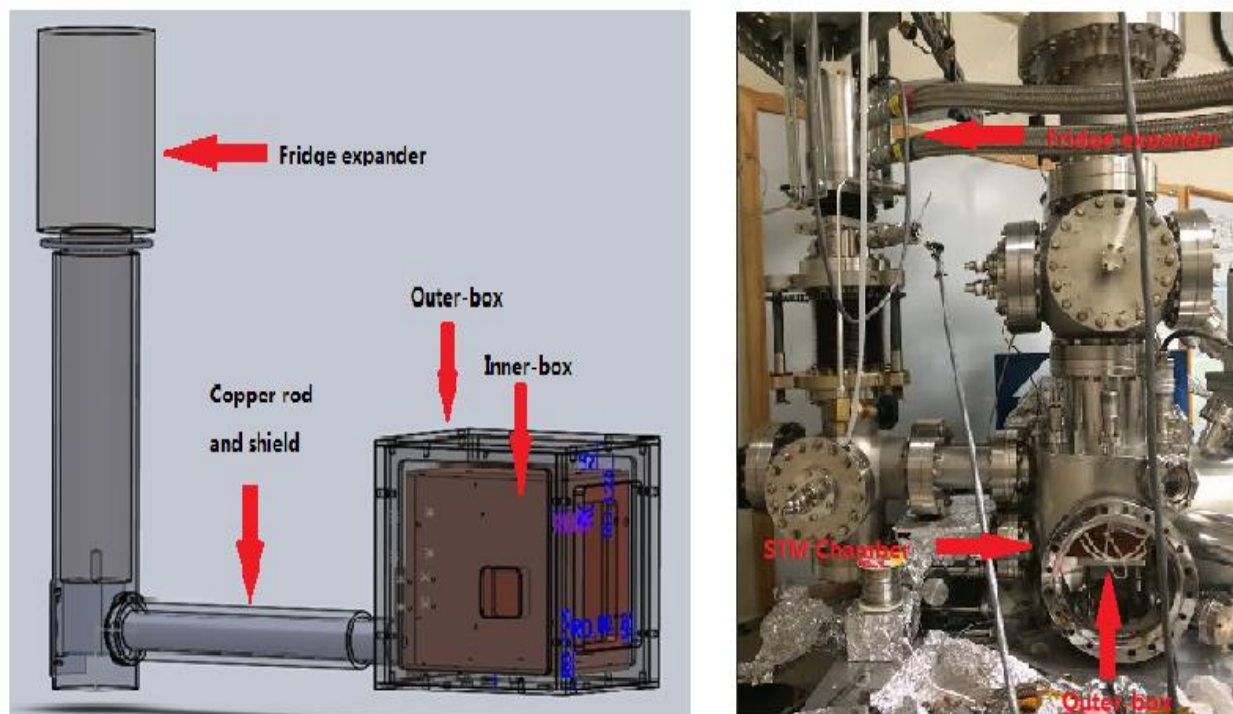


Figure 3.2. Side-view diagram and a photo of the design. The expander was connected to the boxes with a copper rod and a shield. Two boxes were sitting inside the STM chamber. The outer-box was connected to stage 1 at 70 K and inner-box was connected to stage 2 at 4 K of the expander.

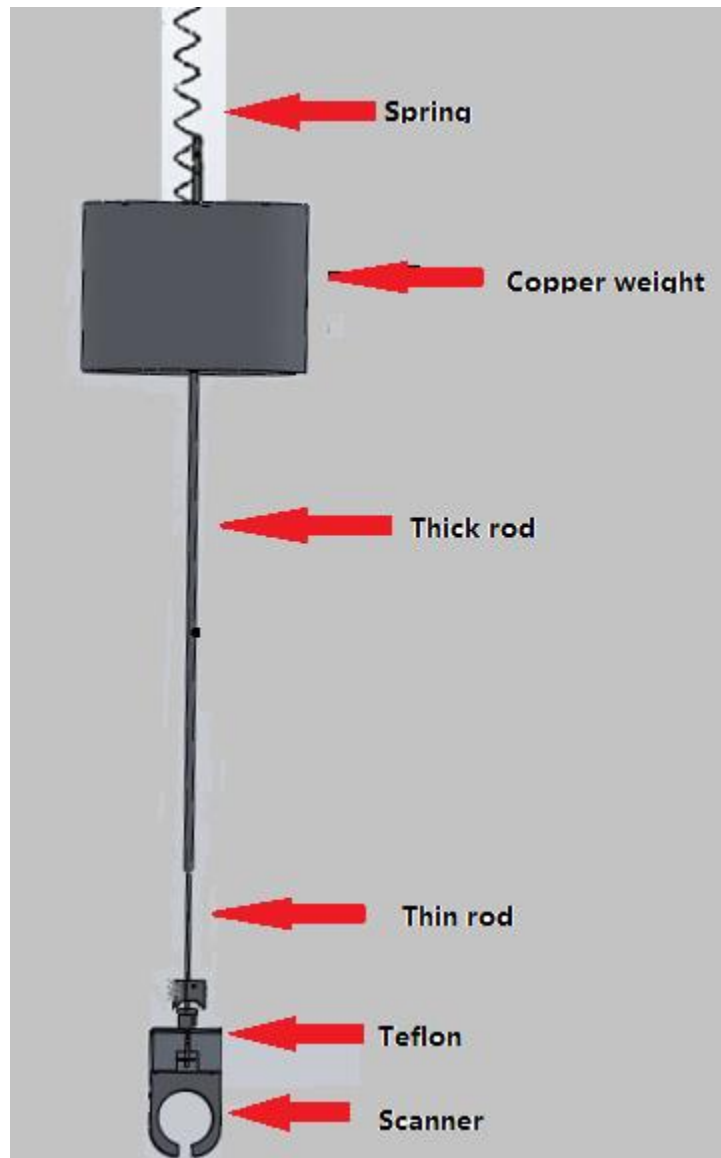


Figure 3.3. Diagram of the suspension mechanism for vibration isolation: a copper weight is attached to a spring to dampen the vibration. A thick rod is attached beneath the weight to increase the stability of the scanner. The thinner rod and the Teflon piece are for minimizing the thermal leakage.

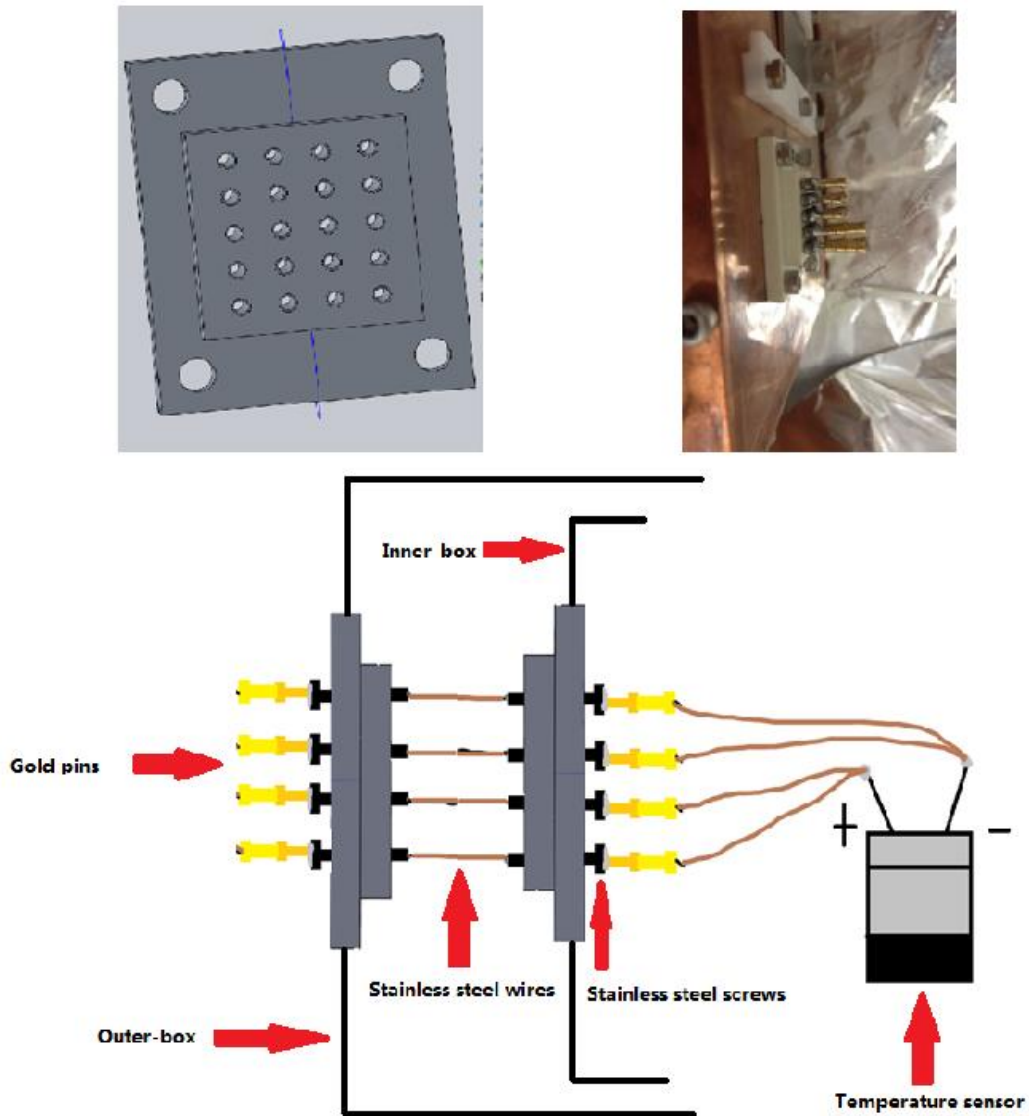


Figure 3.4. Front view, side view of the feedthrough made by Teflon (top) and drawing of the electrical connections from inside of the inner-box to the outside of the outer-box (bottom). The holes in the feedthrough were inserted with stainless steel screws which are connected by Teflon coated stainless steel wires. The other ends of the screws were soldered with gold pins which are easy to plug/unplug with one another.

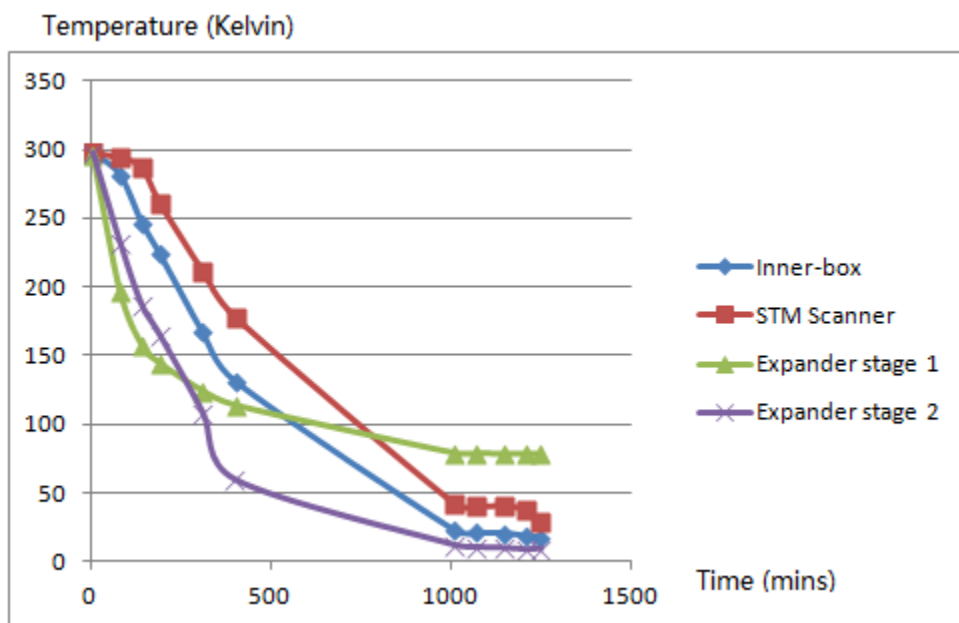


Figure 3.5. Cooling test results with STM scanner and suspension installed. The scanner reached 28 K and the inner-box reached 18 K after the fridge being turned on for 1200 minutes. This 10 K difference was caused by the thermal leakage from the suspension.

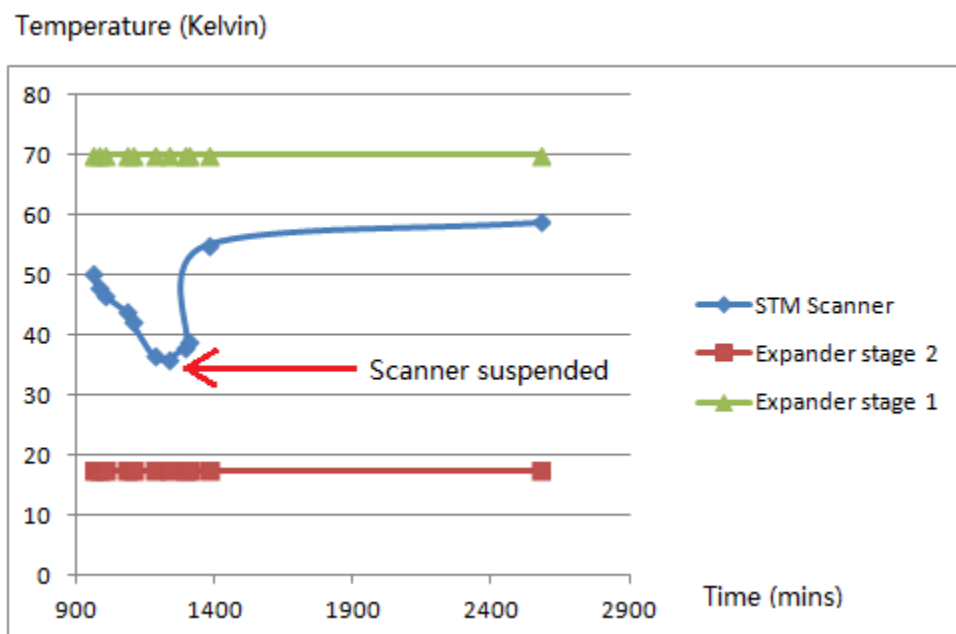


Figure 3.6. Temperature test results with STM scanner being suspended during cooling (with the temperatures of expander stage 1 and 2 staying at 68 K and 17 K). Scanner temperature rose from 35.86 K to 55.03 K within 135 minutes and the equilibrium temperature was ~58 K.

CHAPTER 4

SUMMARY AND OUTLOOK

In summary, large-scale transfer of CVD-grown graphene to clean Si surface in a UHV STM chamber was conducted. A PET/Silicone film was used as the support material for graphene during transfer. SEM and AFM were used to characterize and analyze the transferred graphene. SEM images showed that the ex-situ transfer yield reached 90% and the in-situ transfer yield reached 20% and it can be greatly improved by heating the target sample. AFM images showed that the size of the in-situ transferred graphene could be as large as tens of micrometers squared. This is a first-time demonstration of transferring such large-scale graphene on clean surfaces in UHV. We would like to try transferring graphene to a heated sample next time to get a better graphene yield and continuity. Also we can change the surface energy of the PET film by doing some sort of chemical or physical treatments [64] to improve the transfer result and reduce the residues.

This work could have significant implications in studying graphene-substrate interactions such as understanding the mechanism of graphene serving as an oxidation resistance barrier for clean Si and transparency of graphene to electrons with different energies on an H-passivated Si surface.

For the low temperature STM, with most of the design and construction work done, we were able to do scans at ~30 K with the refrigerator on. With some minor changes to lower the temperature in the future, many interesting experiments can be run using this system such as studying nano-scale water entrapped by graphene [27] and bottom-up fabrication of graphene nano-ribbons in a STM [65].

REFERENCES

- [1] G. E. Moore, "Cramming more components onto integrated circuits," *IEEE Trans. Electron Devices*, vol. 86, no. 1, pp. 82-85, January 1988.
- [2] P. E. Tomaszewski, "Professor Jan Czochralski (1885-1953) and his contribution to the art and science of crystal growth," *American Crystallographic Association*, vol. 27, no. 12 Autumn 1998.
- [3] A. G. Levine, "John Bardeen, William Shockley, Walter Brattain - invention of the transistor - Bell laboratories," *American Physical Society*, 2008. [Online]. Available: <http://www.aps.org/programs/outreach/history/historicsites/transistor.cfm>.
- [4] K. Roy, S. Mukhopadhyay, and S. Member, "Leakage current mechanisms and leakage reduction techniques in deep-submicrometer CMOS circuits," *IEEE Trans. Electron Devices*, vol. 91, no. 2, pp. 305–327, 2003.
- [5] J. G. Ruch, "Electron dynamics in short channel field-effect transistors," *IEEE Trans. Electron Devices*, vol. 19, no. 5, pp. 652–654, May 1972.
- [6] T. Ito and S. Okazaki, "Pushing the limits of lithography," *Nature*, vol. 406, no. 6799, pp. 1027–31, Aug. 2000.
- [7] P. R. Buseck, S. J. Tsipursky, and R. Hettich, "Fullerenes from the geological environment," *Science*, vol. 257, no. 5067, pp. 215–7, Jul. 1992.
- [8] G. Binnig, H. Rohrer and H. R. G. Binnig, "Scanning tunneling microscopy," *IBM J. Res. Dev.*, vol. 30, 1986.
- [9] A. K. Geim, "Graphene: status and prospects," *Science*, vol. 324, no. 5934, pp. 1530–4, Jun. 2009.
- [10] S. Hong and S. Myung, "Nanotube electronics: a flexible approach to mobility," *Nat. Nanotechnol.*, vol. 2, no. 4, pp. 207–8, Apr. 2007.
- [11] M. Shanmugam, R. Jacobs-Gedrim, C. Durcan, and B. Yu, "2D layered insulator hexagonal boron nitride enabled surface passivation in dye sensitized solar cells," *Nanoscale*, vol. 5, no. 22, pp. 11275–82, Nov. 2013.
- [12] A. Javey and J. Kong, *Carbon Nanotube Electronics (Google eBook)*. Springer Science & Business Media, 2009, p. 277.

- [13] A. K. Geim and K. S. Novoselov, "The rise of graphene," *Nat. Mater.*, vol. 6, no. 3, pp. 183–91, Mar. 2007.
- [14] K. S. Novoselov, A. K. Geim, S. V. Morozov, D. Jiang, Y. Zhang, S. V. Dubonos, I. V. Grigorieva, "Electric field effect in atomically thin carbon films," *Science*, vol. 305, no. 5686, pp. 66–68, 2004.
- [15] K. S. Novoselov, A. K. Geim, S. V. Morozov, D. Jiang, M. I. Katsnelson, I. V. Grigorieva, S. V. Dubonos, and A. A. Firsov, "Two-dimensional gas of massless Dirac fermions in graphene," *Nature*, vol. 438, no. 7065, pp. 197–200, Nov. 2005.
- [16] K. I. Bolotin, K. J. Sikes, Z. Jiang, M. Klima, G. Fudenberg, J. Hone, P. Kim, and H. L. Stormer, "Ultrahigh electron mobility in suspended graphene," *Solid State Commun.*, vol. 146, no. 9–10, pp. 351–355, Jun. 2008.
- [17] A. Balandin, S. Ghosh, W. Bao, I. Calizo, D. Teweldebrhan, F. Miao, and C. N. Lau, "Superior thermal conductivity of single-layer graphene," *Nano Lett.*, vol. 8, no. 3, pp. 902–7, Mar. 2008.
- [18] A. Kuzmenko, E. van Heumen, F. Carbone, and D. van der Marel, "Universal optical conductance of graphite," *Phys. Rev. Lett.*, vol. 100, no. 11, p. 117401, Mar. 2008.
- [19] J. U. Lee, D. Yoon, and H. Cheong, "Estimation of Young's modulus of graphene by Raman spectroscopy," *Nano Lett.*, vol. 12, no. 9, pp. 4444–8, Sep. 2012.
- [20] J. Slonczewski and P. Weiss, "Band structure of graphite," *Phys. Rev.*, vol. 109, no. 2, pp. 272–279, Jan. 1958.
- [21] M. O. Goerbig, J. Fuchs, "Theoretical study of graphene in a strong magnetic," 2006. [Online]. Available: <https://www.lps.u-psud.fr/spip.php?article462>.
- [22] Y. C. Chen, D. G. de Oteyza, Z. Pedramrazi, C. Chen, F. R. Fischer, and M. F. Crommie, "Tuning the band gap of graphene nanoribbons synthesized from molecular precursors," *ACS Nano*, vol. 7, no. 7, pp. 6123–8, Jul. 2013.
- [23] X. Li, H. Zhu, K. Wang, A. Cao, J. Wei, C. Li, Y. Jia, Z. Li, X. Li, and D. Wu, "Graphene-on-silicon Schottky junction solar cells," *Adv. Mater.*, vol. 22, no. 25, pp. 2743–8, Jul. 2010.
- [24] A. Gamucci, D. Spirito, M. Carrega, B. Karmakar, A. Lombardo, M. Bruna, A. C. Ferrari, L. N. Pfeiffer, K. W. West, M. Polini, and V. Pellegrini, "Electron-hole pairing in graphene-GaAs heterostructures," Jan. 2014. [Online]. Available: <http://arxiv.org/abs/1401.0902>.

- [25] X. Li, Y. Zhu, W. Cai, M. Borysiak, B. Han, D. Chen, R. D. Piner, L. Colombo, and R. S. Ruoff, "Transfer of large-area graphene films for high-performance transparent conductive electrodes," *Nano Lett.*, vol. 9, no. 12, pp. 4359–63, Dec. 2009.
- [26] A. K. and C. H. Lee, "Synthesis and biomedical applications of graphene: present and future trends," *Advances in Graphene Science*, Jul. 2013. [Online]. Available: <http://www.intechopen.com/books/advances-in-graphene-science/synthesis-and-biomedical-applications-of-graphene-present-and-future-trends>.
- [27] J. D. Wood, "Large-scale growth, fluorination, clean transfer, and layers of graphene and related nanomaterials," Ph.D. dissertation, University of Illinois at Urbana-Champaign, Urbana, IL, 2013.
- [28] Y. C. Lin, C. C. Lu, C. H. Yeh, C. Jin, K. Suenaga, and P. W. Chiu, "Graphene annealing: how clean can it be?" *Nano Lett.*, vol. 12, no. 1, pp. 414–9, Jan. 2012.
- [29] K. T. He, J. D. Wood, G. P. Doidge, E. Pop, and J. W. Lyding, "Scanning tunneling microscopy study and nanomanipulation of graphene-coated water on mica," *Nano Lett.*, vol. 12, no. 6, pp. 2665–72, Jun. 2012.
- [30] S. Bae, H. Kim, Y. Lee, X. Xu, J. S. Park, Y. Zheng, J. Balakrishnan, T. Lei, H. R. Kim, Y. Il Song, Y.-J. Kim, K. S. Kim, B. Ozyilmaz, J.-H. Ahn, B. H. Hong, and S. Iijima, "Roll-to-roll production of 30-inch graphene films for transparent electrodes," *Nat. Nanotechnol.*, vol. 5, no. 8, pp. 574–8, Aug. 2010.
- [31] J. D. Caldwell, T. J. Anderson, J. C. Culbertson, G. G. Jernigan, K. D. Hobart, F. J. Kub, M. J. Tadjer, J. L. Tedesco, J. K. Hite, M. a Mastro, R. L. Myers-Ward, C. R. Eddy, P. M. Campbell, and D. K. Gaskill, "Technique for the dry transfer of epitaxial graphene onto arbitrary substrates," *ACS Nano*, vol. 4, no. 2, pp. 1108–14, Feb. 2010.
- [32] W. Xin, Z. B. Liu, Q. W. Sheng, M. Feng, L. G. Huang, P. Wang, W. S. Jiang, F. Xing, Y. G. Liu, and J. G. Tian, "Flexible graphene saturable absorber on two-layer structure for tunable mode-locked soliton fiber laser," *Opt. Express*, vol. 22, no. 9, p. 10239-10247, Apr. 2014.
- [33] M. Liu, "Characterization study of bonded and unbonded polydimethylsiloxane aimed for bio-micro-electromechanical systems-related applications," *J. Micro/Nanolithography, MEMS, MOEMS*, vol. 6, no. 2, p. 023008, Apr. 2007.
- [34] Y. Yu Wang and P. J. Burke, "A large-area and contamination-free graphene transistor for liquid-gated sensing applications," *Appl. Phys. Lett.*, vol. 103, no. 5, p. 052103, 2013.
- [35] R. W. R. L. Gajasinghe, S. U. Senveli, S. Rawal, A. Williams, A. Zheng, R. H. Datar, R. J. Cote, and O. Tigli, "Experimental study of PDMS bonding to various substrates for monolithic microfluidic applications," *J. Micromechanics Microengineering*, vol. 24, no. 7, p. 075010, Jul. 2014.

- [36] X. D. Chen, Z. B. Liu, C. Y. Zheng, F. Xing, X. Q. Yan, Y. Chen, and J. G. Tian, "High-quality and efficient transfer of large-area graphene films onto different substrates," *Carbon N. Y.*, vol. 56, pp. 271–278, May 2013.
- [37] D. Petrovykh, "Silicon nanoworld: scanning tunneling microscopy basics," 2008. [Online]. Available: <http://nanowiz.tripod.com/stmbasic/stmbasic.htm>.
- [38] R. M. Feenstra, J. A. Stroscio, and A. P. Fein, "Tunneling spectroscopy of the Si(111)2 × 1 surface," *Surf. Sci.*, vol. 181, no. 1–2, pp. 295–306, Mar. 1987.
- [39] K.A. Ritter and J. W. Lyding, "Characterization of nanometer-sized, mechanically exfoliated graphene on the H-passivated Si(100) surface using scanning tunneling microscopy," *Nanotechnology*, vol. 19, no. 1, p. 015704, Jan. 2008.
- [40] K. A. Ritter and J. W. Lyding, "The influence of edge structure on the electronic properties of graphene quantum dots and nanoribbons," *Nat. Mater.*, vol. 8, no. 3, pp. 235–42, Mar. 2009.
- [41] P. M. Albrecht and J. W. Lyding, "Ultrahigh-vacuum scanning tunneling microscopy and spectroscopy of single-walled carbon nanotubes on hydrogen-passivated Si(100) surfaces," *Appl. Phys. Lett.*, vol. 83, no. 24, p. 5029, Dec. 2003.
- [42] K. T. He, "Characterization of graphene-substrate interactions using scanning tunneling microscopy," Ph.D. dissertation, University of Illinois at Urbana-Champaign, Urbana, IL, 2013.
- [43] K. T. He, J. C. Koepke, S. Barraza-Lopez, and J. W. Lyding, "Separation-dependent electronic transparency of monolayer graphene membranes on III-V semiconductor substrates," *Nano Lett.*, vol. 10, no. 9, pp. 3446–52, Sep. 2010.
- [44] X. Liu, "Design of a low-temperature, ultrahigh-vacuum scanning tunneling microscope," B.S. thesis, University of Illinois at Urbana-Champaign, Urbana, IL, 2011.
- [45] M. Morita, T. Ohmi, E. Hasegawa, M. Kawakami, and M. Ohwada, "Growth of native oxide on a silicon surface," *J. Appl. Phys.*, vol. 68, no. 3, p. 1272, 1990.
- [46] S. Chen, L. Brown, M. Levendorf, W. Cai, S. Y. Ju, J. Edgeworth, X. Li, C. W. Magnuson, A. Velamakanni, R. D. Piner, J. Kang, J. Park, and R. S. Ruoff, "Oxidation resistance of graphene-coated Cu and Cu/Ni alloy," *ACS Nano*, vol. 5, no. 2, pp. 1321–7, Feb. 2011.
- [47] M. Schriver, W. Regan, W. J. Gannett, A. M. Zaniwski, M. F. Crommie, and A. Zettl, "Graphene as a long-term metal oxidation barrier: Worse than nothing," *ACS Nano*, vol. 7, no. 7, pp. 5763–8, Jul. 2013.
- [48] "REVALPHA Thermal Release Semiconductor Tape-NItto." [Online]. Available: <http://www.nittousa.com/files/ProductDetails.aspx?Pid=442>.

- [49] "Amazon.com: SUPERSHIELDZ- Anti-Glare & Anti-Fingerprint (Matte) Screen Protector For iPhone 5 5S 5C + Lifetime Replacements Warranty [6-PACK] - Retail Packaging: Cell Phones & Accessories." [Online]. Available: <http://www.amazon.com/SUPERSHIELDZ-Anti-Glare-Anti-Fingerprint-Protector-Replacements/dp/B00EOYMO66>.
- [50] W. Gao, P. Xiao, G. Henkelman, K. M. Liechti, and R. Huang, "Interfacial adhesion between graphene and silicon dioxide by density functional theory with van der Waals corrections," *J. Phys. D. Appl. Phys.*, vol. 47, no. 25, p. 255301, Jun. 2014.
- [51] Marton and Kati, *Vacuum Physics and Technology (Google eBook)*. Academic Press, 1980, p. 592.
- [52] W. Kern, "The evolution of silicon wafer cleaning technology," *J. Electrochem. Soc.*, vol. 137, no. 6, p. 1887, 1990.
- [53] *Princeton University Lab Manual, Section 10: Chemical specific information — Piranha solutions*. Princeton University, 2014. [Online]. Available: <http://web.princeton.edu/sites/ehs/labsafetymanual/cheminfo/piranha.htm>.
- [54] D. J. Chadi, "Atomic and Electronic Structures of Reconstructed Si(100) Surfaces," *Phys. Rev. Lett.*, vol. 43, no. 1, pp. 43–47, Jul. 1979.
- [55] P. N. Incze, Z. E. Horváth, K. Kamarás, and L. P. Biró, "Measuring the correct thickness of graphene layers by intermittent contact atomic force microscopy," vol. 1, pp. 273–274, 2009.
- [56] J. Kang, S. Hwang, J. H. Kim, M. H. Kim, J. Ryu, S. J. Seo, B. H. Hong, M. K. Kim, and J.-B. Choi, "Efficient transfer of large-area graphene films onto rigid substrates by hot pressing," *ACS Nano*, vol. 6, no. 6, pp. 5360–5, Jun. 2012.
- [57] T. Mashoff, M. Pratzer, and M. Morgenstern, "A low-temperature high resolution scanning tunneling microscope with a three-dimensional magnetic vector field operating in ultrahigh vacuum," *Rev. Sci. Instrum.*, vol. 80, no. 5, p. 053702, May 2009.
- [58] S. H. Pan, E. W. Hudson, J. C. Davis, "He refrigerator based very low temperature scanning tunneling microscope," *Rev. Sci. Instrum.*, vol. 70, no. 2, 1999.
- [59] B. C. Stipe, M. A. Rezaei, and W. Ho, "A variable-temperature scanning tunneling microscope capable of single-molecule vibrational spectroscopy," *Rev. Sci. Instrum.*, vol. 70, no. 1, p. 137, Jan. 1999.
- [60] N. Moussy, H. Courtois, and B. Pannetier, "A very low temperature scanning tunneling microscope for the local spectroscopy of mesoscopic structures," *Rev. Sci. Instrum.*, vol. 72, no. 1, p. 128, Jul. 2001.

- [61] "Thermal conductivity of some common materials and gases," [Online]. Available: http://www.engineeringtoolbox.com/thermal-conductivity-d_429.html.
- [62] "ShapalTM-M - Ceramics - Research Materials - Goodfellow USA," [Online]. Available: <http://www.goodfellowusa.com/larger-quantities/ceramics/shapal-m/>.
- [63] "Conduction - The physics hypertextbook," 1998. [Online]. Available: <http://physics.info/conduction/>.
- [64] Enercon Industries Corp., "Corona treating for coating applications," Faustel, Inc., WI. [Online]. Available: <http://www.faustel.com/technical-library/corona-treating-for-coating-applications/>.
- [65] J. Cai, P. Ruffieux, R. Jaafar, M. Bieri, T. Braun, S. Blankenburg, M. Muoth, A. P. Seitsonen, M. Saleh, X. Feng, K. Müllen, and R. Fasel, "Atomically precise bottom-up fabrication of graphene nanoribbons," *Nature*, vol. 466, no. 7305, pp. 470–3, Jul. 2010.